

CHAPTER I

INTRODUCTION

1.1 Research Background

In the recent manufacturing field, parts fabrication is accomplished by conservative means, or called traditional machining. Processes such as turning, milling, boring, grooving, and lathe are the most common processes in manufacturing. These processes are also known as subtractive manufacturing process, due to the mechanism of removing material in order to obtain the final shape of the part. This process, however, contributing to the chip build-up, results in waste produced, hence messy workplace.

Rapid prototyping (RP) is a new manufacturing process in non-traditional machining (NTM) category. It is a process by means of layer-by-layer mechanism, until the part completely fabricated. This process is also known as additive manufacturing, due to the said mechanism. Generally, the machine receives the input by importing the drawing file in STL format into the software, and then it will be transferred into the machine drive. Next, the machine will create the part by following the exact geometry of the part from the first layer, before moving to the next consecutive layers. Post-processing also will be neglected, as this process produced a ready-made product, which

means it can be used straight away right after the fabrication process completed. Hence, there will be no chip build-up, results in a neat and safe workplace, as well as save time.

There are three categories that fall under RP machining. They are liquid-based, solid-based, and powder-based RP systems. For liquid-based RP system, stereolithography (SLA), and solid ground curing (SGC) are the examples of the processes. This system has an initial form of the material in liquid state. Both of the processes are using ultra-violet (UV) light in the curing process of the part, in which the liquid is converted to the solid states. Fused deposition modeling (FDM), and laminated object manufacturing (LOM) are some of the examples for solid-based RP system. The raw material will be heated and changed to a molten state, before extruding through the nozzle and solidified as final part for FDM, meanwhile for LOM uses cutting and gluing until the part is fabricated. Lastly, examples of powder-based RP system are selective laser sintering (SLS), three-dimensional printing (3DP), and laser engineered net shaping (LENS). This system uses binder as the agent to bind the powder raw material into a solid and compact final part.

In RP, quality of the fabricated part is always being the main priority. In order to achieve the best quality, there are several process parameters that taken into consideration before proceed with the fabrication process. They are air gap, raster orientation, raster angle, layer thickness, and model temperature. These parameters can be varies depending on the model of RP machine to get the best parameters that results in good surface finish, and high strength and stiffness.

1.2 Problem Statement

Rapid prototyping technology is becoming more popular in fabricating parts, especially FDM . However, the initial cost of the machine is really expensive, as well as the material. Nowadays, there are some developed low-cost FDM machines by various manufacturers, that widely used by hobbyist, artists, and even the public. The low-cost FDM allows fabrication of small parts either for leisure time or even for spare parts. The reliability of the low-cost FDM is yet to be checked by several mechanical tests such as tensile and compression tests. With these experiments, the low-cost FDM can be determined either it is suitable to be used to fabricate parts or vice versa.

1.3 Objectives

The objectives of this project can be summarized as follows:

- 1) To investigate the effect of layer thickness and infill material percentage on the ultimate tensile stress and the ultimate compressive stress of the parts.
- 2) To compare the performance of commercial and low-cost FDM machines, while compare with the performance of the specimens fabricated using plastic injection molding machine.
- 3) To determine the reliability of the low-cost FDM machine in parts fabrication.

1.4 Scope of Research

In this research, the main purpose is to determine the reliability of low-cost FDM machine. This will be done by preparing specimens using both commercial and low-cost FDM machines. Some specimens will also be fabricated using the plastic injection molding machine, just to get a benchmark result for both the FDM machines

fabricated specimens. Two process parameters will be varies in preparing the specimens which are infill material percentage and layer thickness. Air gap, raster angle, and model temperature will be fixed for all specimens. Material used for all specimens is ABS. After all the specimens prepared, they will be undergoes several tests such as tensile test and compression test. Results will be gathered, and discussion and conclusion will be finalized.

1.5 Significant of the Project

The comparison made in this project will show the percentage of reliability of the low-cost FDM machine compared to the commercial one. From the results of the tests, it will clearly show the level of reliability of the low-cost FDM printer, especially in the fabrication of small products. Hence, huge amount of initial cost in RP might be avoided.

CHAPTER II

LITERATURE REVIEW

2.1 Overview of Rapid Prototyping

Rapid Prototyping (RP) technology is widening nowadays in the advanced manufacturing process field. This is due to the special features of RP and the ease of operation. The name itself shows that this is a fast process in manufacture the products, and also a low cost manufacturing process of a small series of components (J. Czyżewski, 2009). This technology can be considered as a new foundation in the manufacturing field, due to the ability to eliminate post-processing stage, a clean and smooth process, a safe way to manufacture products, and the ability to create ready-to-use final products. This process refers to the fabrication of a physical, three-dimensional part of arbitrary shape directly from a numerical description, typically a CAD model, by a quick, totally automated, and highly flexible process (Noorani, 2006). This technique is one of the most promising techniques to reduce product development time by a way of realizing the prototype that can be used directly in assemblies, product testing, or tooling for short or medium run production (R. Anitha, 2001). This process is an additive process, whereby the product is created layer by layer until the whole product finished. RP also is known as freeform fabrication (FFF). The ideas of using RP are to

increase effective communication, to decrease development time, to decrease costly mistakes, and to minimize sustaining engineering changes.

RP is also known as an additive manufacturing, where this technology adding material to build final parts, instead of subtracting material which results in waste production. The material is deposited layer-by-layer in a specific height of each layer set in the software before printing process, and follows the shape of the desired part. Shown below is the mechanism of layer-by-layer additive manufacturing process in FDM.

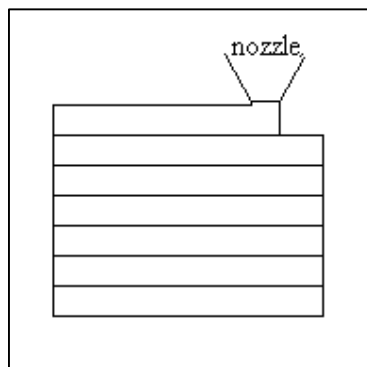


Figure 2.1: Layer-by-Layer Mechanism

Due to these advantages, there are many applications from various fields that using RP such as functional prototype development (Y.G. Im, 2007), medical applications (Giorgio Colombo, 2010; S. Lohfeld, 2007; Suman Das, 2003), automobile industries (B. Wiedemann, 1999), construction industries (R.A. Buswell, 2007), space instrument development (P. Rochusa, 2007), die making (Zhang Yu, 2009), wind tunnel model (S. Daneshmand, 2008), dentistry (Abbas Azari, 2009), and many more. When it comes to layer-by-layer mechanism, there is a common limitation in RP called stair-step effect. This effect is closely related to the surface quality of the fabricated part. As a result of this effect, the appearance of details whose dimension are in the order of layer thickness is significantly altered (Armilotta, 2006).

In RP, there are general steps will be taken in the manufacturing process of a part. The first step in RP is the creation of CAD file of the part to be produced. The

complete drawing file must be in solid or 3D, and a conversion into STL file is necessary. STL format stands for stereolithography, which is triangulated representation of a solid model, and usually stored in binary format to conserve disk space. Some RP machine requires pre-processing of the STL file, which is slicing, parameters setup such as temperature control, layer thickness, and printing speed. Once finished, the file will be transferred into the controller board of the RP machine, and the machine starts to produce the part. After some times, depending on the complexity of the shape, the part is completely produced, and sometimes requires post-processing for cleaning and refining the part, and then the part can be used. Figure below shows the RP cycle for a complete manufacturing process.

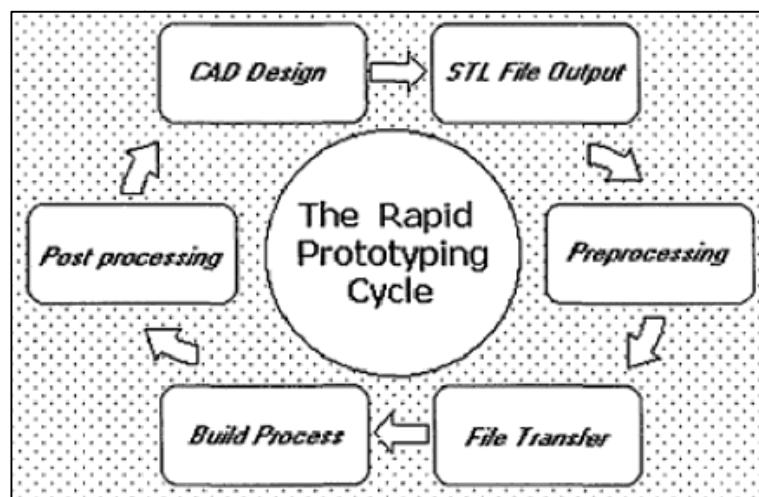


Figure 2.2: RP Cycle Begins with CAD Design (Cooper, 2001)

However, a part with a protruding section requires supporting structure. There are several types of supporting structure can be used depending on the shape of the part. The most common supporting structures used in RP are gussets, ceiling, ceiling within an arch, and island. Once the printing process completed, the supporting structure will be removed from the final part. Shown below are the types of the mentioned supporting structures.

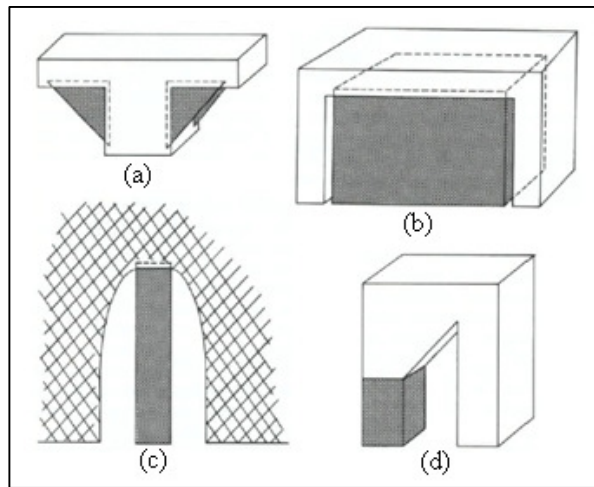


Figure 2.3: Supporting Structures: (a) Gussets, (b) Ceiling, (c) Ceiling within an Arch, and (d) Islands (Jacobs, 1992)

The gussets support structure is used at cantilevered section. An overhang that extends beyond 1.27 mm will reveal curl when unrestrained. Gussets are the triangular shaped supports that are strong, easily removed, and are efficient with respect to STL file size. Gussets should extend into the walls by approximately 0.38 mm in order to ensure a solid attachment. Ceiling and ceiling within an arch support structures are usually used when a down-facing overhang area occurs in the middle of the part to be produced, usually longer than 1.27 mm. A feature that slopes between $0^{\circ} - 30^{\circ}$ from horizontal is also considered as a flat, down-facing area, hence support is required. The islands support structure are layers of the part geometry that would otherwise be unconnected to any other section of the part. They must be anchored to the platform or to the part itself, and can be connected to the prior layers of the part, providing the structure is rigid (Jacobs, 1992).

RP systems can be divided into three categories, which are categorized by the initial form of the raw material used for the process, and the method of producing the final product. These categories are liquid-based, solid-based, and powder-based RP systems. Liquid-based RP systems have an initial form of its raw material in liquid state. The liquid state will be converted to solid state by curing process in the RP

systems. Some of the RP systems that fall into this category are 3D Systems' stereolithography (SLA), Objet Geometries Ltd.'s Polyjet, and Cubital's solid ground curing (SGC). 3D Systems' SLA uses ultraviolet (UV) laser, Objet Geometries's Polyjet uses a UV lamp via jetting head, and Cubital's SGC uses UV masked lamp for the curing process of the product.

Similar to liquid-based RP systems, solid-state RP systems are categorized from the solid state of its initial raw material used in the systems. The solid state raw material can be in the form of filaments, wires, rolls, laminates, or pellets. Stratasys' fused deposition modeling (FDM), Cubic Technologies' laminated object manufacturing (LOM), and 3D Systems' multi-jet modeling (MJM) system are the common example of RP systems under this category. Stratasys' FDM and 3D Systems' MJM use melting and fusing method, while Cubic Technologies' LOM uses cutting and gluing method.

The last category is powder-form RP systems, which is solid, but intentionally created as a different category based on the shape of the raw material – grain-like form. The RP systems that fall under this category are 3D Systems' selective laser sintering (SLS), Z Corporation's three-dimensional printing (3DP), and Optomec's laser engineered net shaping (LENS). As in the name of the systems, 3D Systems' SLS and Optomec's LENS use laser as the binder between the powder particles, while Z (3DP) uses glue as the binder to form the object (Chua Chee Kai, 2010). Some of the processes acquire no post-processing, and the final product manufactured can straight away be used. In general, the raw materials used in RP are glue-backed paper for LOM, plastic spool for FDM, plastic or metal powder for 3D printer and SLS, and liquid resin for SLA.

2.2 Fused Deposition Modeling (FDM)

Fused deposition modeling (FDM) is an additive manufacturing technology commonly used for modeling, prototyping, and batch production. This type of RP uses computer aided design (CAD) based automated additive manufacturing process to construct parts that are used directly as finished products or components (Singh, 2012). In FDM, the raw material used is plastic filament rolled on a spool. The filament will be extruded by the extruder mechanism to the heater element, and will be melted before extruding through the nozzle. As the material is deposited onto the build envelope, it cools, solidifies, and bonds with the adjoining material. After one layer completely deposited, the build envelope will move downward at certain preset height, and the next layer will be deposited. This process is repeated until the part completely printed. The figure below shows the schematic diagram of FDM machine.

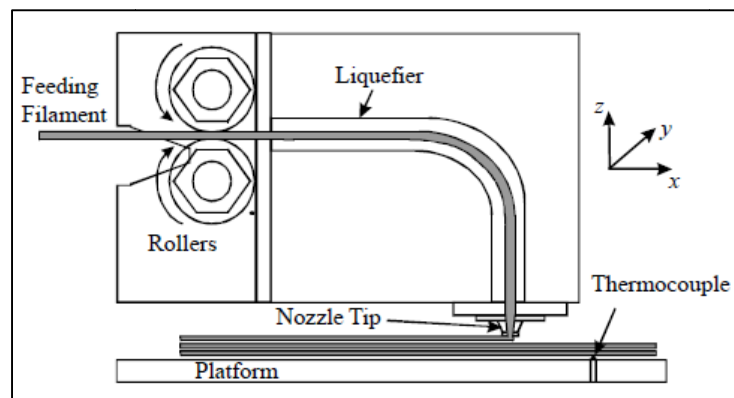


Figure 2.4: Schematic Diagram of FDM Machine and Filament Deposition Process (Q. Sun, 2008)

The material used in FDM usually is thermoplastic filament, and acrylonitrile butadiene styrene (ABS) plastic is the most common material. ABS is a carbon chain copolymer and belongs to styrene ter-polymer chemical family. It is made by dissolving butadiene-styrene copolymer in a mixture of acrylonitrile and styrene monomers and then polymerizing the monomers with free-radical initiators. It contains 90 – 100% acrylonitrile/butadiene/styrene resin and may also contain mineral oil (0 – 2%), tallow

(0 – 2%), and wax (0 – 2%). Its three structure units provide a balance of properties with the acrylonitrile providing heat resistance, butadiene imparting good impact strength, and the styrene gives the copolymer its rigidity (Anoop Kumar Sood, 2010). The other materials that can be considered are polylactic acid (PLA), high density polyethylene (HDPE), low density polyethylene (LDPE), polypropylene (PP), unplasticized polyvinyl chloride (UPVC), and acrylic (also known as PMMA).

FDM process has the ability to produce parts with the high complexity of geometry. This is the main advantage of this process, which is hard to achieve by conservative manufacturing process means. In addition of this process, most of the time, the part produced requires no post-processing, or just a simple cleaning or finishing for the part. In order to produce small parts, multiple parts can be produced in a single printing process using FDM, thus, this process is really save time.

However, the initial cost of FDM process is really high, based on commercial FDM machine price, for example Dimension printer, which is ranged from \$24, 900 to \$32, 900 (Dimension; Dimension), and varies price range for other printers. FDM machine also requires expert in order to operate the machine, to avoid any unwanted accidents.

Due to these disadvantages, Evan *et. al* designed a cheap and simple personal desktop fabricator kit, and named it Fab@Home printer Model 1 circa 2007. They are experimenting the printer by placing it in the hand of hobbyists, inventors, and artists. As a result, this printer can be used by using various types of materials with low melting point. Some materials that proven can be used by the printer are chocolate, silicone rubber, wax, and bismuth metal alloy (Evan Malone, 2007). Basically, the Fab@Home Model 1 printer is a three-axis Cartesian gantry positioning system driven by stepper motors attached to lead screws. The material deposition mechanism is based on syringe-

based extrusion tool which uses a linear stepper motor to control the syringe plunger position. Similar to other available FDM machine, this printer obtains input from STL file, generate and execute tool paths in order to fabricate the parts or objects.

Along with the development of Fab@Home Model 1, there are several manufacturers fabricated their low-cost RP machine. RepRap, Bits From Bytes, MakerBot Industries, and Ultimaking Ltd., are some examples of the mentioned manufacturers. RepRap with their RP named Mendel is a do-it-yourself 3D printer, which the printer parts can be bought separately from various suppliers or local store. A printer kit called RapMan 3.2 from Bits From Bytes is another example of this low-cost RP machine. Similar with RepRap, RapMan 3.2 is also a do-it-yourself printer. However, it has a better appearance than RepRap. Currently, Bits From Bytes became part of the 3D Systems family in October 2010. In the meantime, 3D Systems also commercialized their own low-cost RP machine called 3DTouch.

MakerBot Industries and Ultimaking Ltd. are the most popular manufacturers of low-cost RP machine these days, called Replicator and Ultimaker respectively. Both have a kit made of wood and have the size of a desktop printer. They use wooden body because of its durability, and light-weight. Replicator by MakerBot has dual extruder for different color materials, or used for support material extruder. Ultimaker by Ultimaking Ltd. has one extruder, and the second extruder comes separately, and can be attached later. MakerBot Industries however, recently introduced their brand new printer called Replicator 2, with an even more attractive appearance, and more precise on z-axis resolution. However, this model is only optimized for PLA material, as mentioned in their website. All these models mentioned for the low-cost RP machine are using plastic filament, melted using heater element, and extruded through the nozzle to make the parts, which is the fundamental of FDM machine. Shown below are the examples of the small-scale FDM printers.

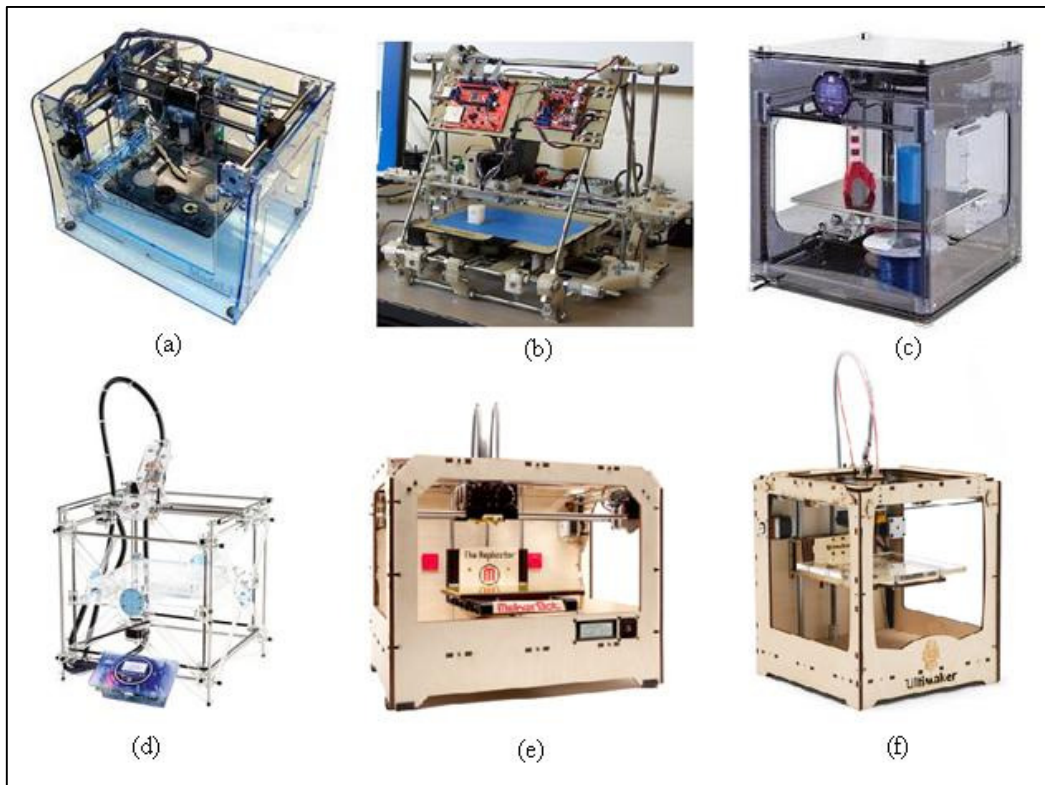


Figure 2.5: Small-Scale FDM Printers: (a) Fab@Home Model 1, (b) RepRap, (c) 3DTouch, (d) RapMan 3.2, (e) MakerBot “The Replicator”, and (f) Ultimaker

2.3 Process Parameters

In FDM, the most important things should be considered are the parts quality in terms of surface roughness, solidity, strength, and reliability. Even though FDM can make it ease and fast in fabricating parts, it also must meet the said factors. It will be very convenient to have a machine that can fabricate parts faster even with high complexity, in the same times meets these factors. For that, there are some previous research works from various good researchers in FDM. In general, they are considering several vital process parameters and test them through several experiments. Raster orientation, raster angle, air gap, bead width, color, and model temperature are the most common parameters that are taken into consideration in FDM.

2.3.1 Raster Orientation

This term refers to the inclination of the part in a build platform with respect to X, Y, and Z axis. X and Y axis are considered parallel to build platform and Z-axis is along the direction of part builds. In other word, the orientation of a part refers to the build direction during the fabrication of the part. Several factors should be considered in deciding the suitable build direction of the part to be fabricated. The main factor is the shape of the part. For an instance, in fabricating a cylinder shape part, it is more suitable to put it vertically in the software before starting with the fabrication process, instead of horizontal. Refer figure below for a clearer view of the building direction applied in FDM.

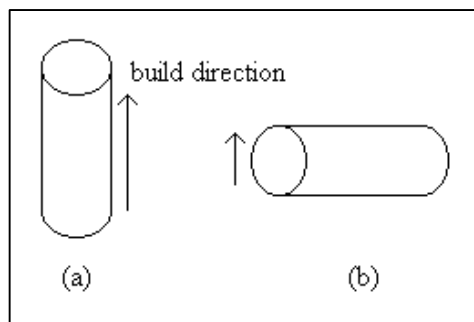


Figure 2.6: Build Direction for Cylindrical Shape Part in Different Orientation: (a) Vertical, and (b) Horizontal

From the figure above, the arrow indicates the build direction of the part. As mentioned earlier, this part is more suitable to put the part vertically during the experiment set up as shown in (a), rather than horizontally as shown in (b). This is because, orientation shown in (b) will require supporting structure in fabricating the part, that results in more material usage, post-processing of removing the support material, and surface finishing. Hence, the fabricating process is time consuming.

Sung-Hoon Ahn *et. al* examines the process parameters of FDM (Sung-Hoon Ahn, 2002), and raster orientation is one of them. From their experiment, this parameter

was examined for the compression test. They fabricated specimens with two different build directions as shown in the figure above, fixed raster angle of $45^{\circ}/-45^{\circ}$ and zero air gap for transverse and axial specimens. As a result, the strength is ranged 80 – 90% of those for injection molded.

There was also another experiment conducted by C. S. Lee *et. al* on build direction parameter for compression test for FDM, nano composite deposition system (NCDS), and 3D printer (3DP). In fact, it was the only parameter taken into consideration for the test. They had specimens with axial (horizontal) and transverse (vertical) directions for FDM. They observed that the axial FDM specimen's compressive strength was 41.26 MPa, which was 11.6% higher than the transverse FDM specimen's. From their results, they concluded that build direction caused the anisotropic behavior of RP parts, and eventually their compressive strength was changed by anisotropic behavior (C. S. Lee, 2007).

2.3.2 Raster Angle

Raster angle is the angle set on applying infill pattern during the fabrication process in FDM. Usually, $45^{\circ}/-45^{\circ}$ angle is used in fabricating parts. However, there are several raster angle patterns that also can be applied during the fabrication process such as 0° , 90° , and $0^{\circ}/90^{\circ}$. These raster angle patterns can be varies depend on the application of the part to be fabricated. The raster angle patterns can be seen in the figure below.

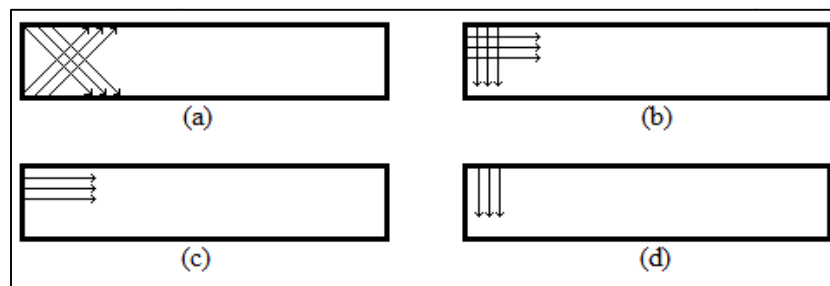


Figure 2.7: Raster Angle Patterns of (a) $45^{\circ}/-45^{\circ}$, (b) $0^{\circ}/90^{\circ}$, (c) 0° , and (d) 90°

For certain shape of part like cylinder part, those raster angle patterns also can be used. At the same time, there are several patterns that could take into consideration such as hilbertcurve, archimedeanchords, and octagramspiral. However, these patterns are not easily available in all software to operate the FDM machine, especially in the open source software. To date, there is one software which these patterns are available, named ReplicatorG. Even though it is freeware, calibrating the FDM with this software is not easy. Trial-and-error is needed to calibrate the printer using this software until it is ready to print. Shown below are the examples of the said patterns.

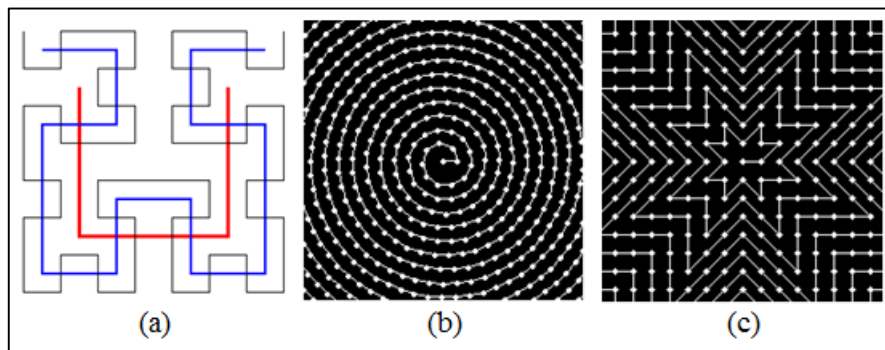


Figure 2.8: Patterns Available in ReplicatorG Software: (a) Hilbertcurve ("Hilbertcurve,"), (b) Archimedeanchords ("Math-PlanePath Gallery,"), and (c) Octagramspiral ("Math-PlanePath Gallery,") Patterns

There is also another popular open-source software for small scale FDM printer called Cura. In this software, the raster angle is set default to 45° / -45° . This is because, the founder of this software created it by means of simplification for the user to operate their small scale FDM printer with no or less problem. However, there are also some patterns that can be used only to fabricate hollow objects called rectangular grid, circular grid, and hexagonal grid or honeycomb, as shown below.

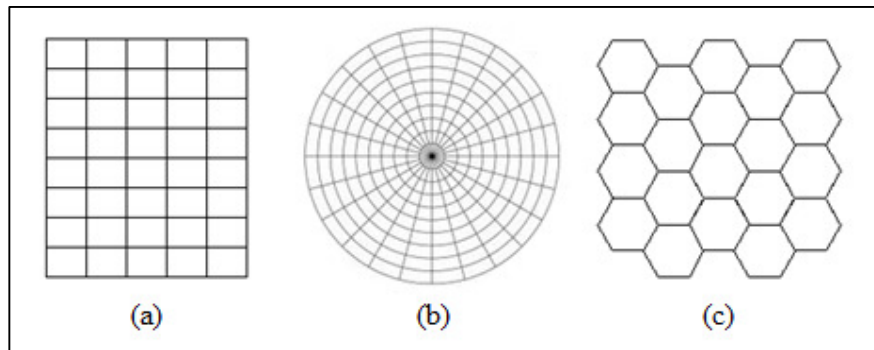


Figure 2.9: Patterns Available in Cura Software: (a) Rectangular Grid, (b) Circular Grid, and (c) Hexagonal Grid or Honeycomb

Rupinder Singh investigated properties of plastic replicas fabricated as small sized product molds with FDM (Singh, 2012). He found that 0° inclination orientation (horizontal) produced best morphology hence used for final experimentation. Surface roughness measured was around $1.21 - 1.24 \mu\text{m}$ (Ra). Hardness measured as per ASTM D2240 testing standard around 78 – 81 shore hardness. Horizontal orientation is the most cost effective and gives best dimensional accuracy.

ASTM D2240 allows for hardness measurement on rubber specimen using a specified standard indenter. There are several hardness measurement scales (A, B, C, D, DO, O, OO, and M), and used to evaluate the indentation hardness of materials such as elastomers, thermoplastic elastomers, vulcanized rubber, cellular, gel-like, and plastics. By using a hardened steel indenter, the specimen will be indented with specific geometry and force, based on the chosen scale of measurements. The measured data will be converted into hardness number ranged from 0 to 100 (Bruker).

There was also a research on examining the effect of layer orientation on the mechanical properties of rapid prototype ABS P400 specimens by performing tensile, three-point bending, and impact tests by Es-Said *et. al* (O. S. Es-Said, 2000). In their study, specimens with five types of orientations were fabricated, which are 0° , $45/-45^\circ$, 45° , 90° , and $45/0^\circ$ orientations. From their results, highest ultimate and yield strengths

in 0° orientation, followed by $45/0^\circ$, $45/-45^\circ$, 90° , and 45° orientations in descending order for tensile test, 90° and 45° orientations having almost same results. Delamination occurred along layer interface, caused by weak interlayer bonding and/or interlayer porosity. For 3-point bending test, highest modulus of rupture value was in the 0° orientation followed by the equivalent values in the $45/-45^\circ$, $45/0^\circ$, and 45° orientations, followed by 90° orientation. Lastly for Izod impact test, 0° orientation had the highest absorbed energy values prior to fracture by an order of magnitude over the 90° orientation, and the other orientations are equivalent.

From a recent research by Fatimatuzahraa *et. al*, they were experimenting with two types of raster angle which are crisscrossed ($45^\circ/-45^\circ$), and cross ($0^\circ/90^\circ$). They predicted that crisscross direction will gives higher mechanical properties compared to the cross direction. Four types of experiment were conducted such as tensile test, deflection test, flexural test, and impact test. From all the results, they concluded that crisscross specimen has higher strength value for deflection test, flexural test, and impact test. For tensile test, they claimed that the sample got higher surface roughness at the edge of the crisscross specimen, causing it to fracture so easily (A.W. Fatimatuzahraa, 2011).

2.3.3 Air Gap

Another factor affecting the performance of the printed part by using FDM is the air gap. The air gap is defined as the gap between each consecutive extruded molten plastic within the same layer. There are three types of air gap which are negative air gap, zero air gap, and positive air gap. When the extruded molten plastic within the same layer overlap each other, this is called the negative air gap. Zero air gap is when the material is extruded and placed side by side without overlapping each other. Lastly, for positive air gap, there is a gap between the molten plastic extruded in the same layer,

and results in the porous structure of the specimen. Shown below are the types of air gap that can be applied in FDM.

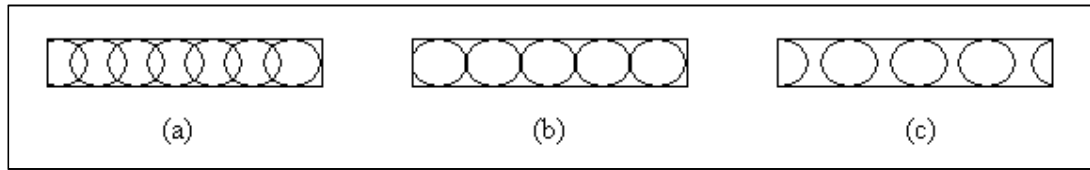


Figure 2.10: Types of Air Gap: (a) Negative, (b) Zero, and (c) Positive Air Gaps

There is a researcher investigating the effects of air gap in FDM by Espalin *et. al* (David Espalin, 2010). They were investigating the use of medical grade PMMA in FDM to fabricate porous customized freeform structures for several applications including craniofacial reconstruction and orthopedic spacers. Then they were examining the effects of different fabrication conditions on porosity and mechanical properties of PMMA specimens. In their experiments, they found that the stiffness and the yield strength of the specimens decreased when porosity increased. For demonstration purpose, they successfully fabricated patient-specific, 3D PMMA implants with varying densities, including cranial defect repair and femur models by using FDM.

2.3.4 Layer Thickness

Another factor that affects the part performance is the layer thickness applied during the fabrication process. Layer thickness factor is closely related to the time consumption of the fabrication process. This is because, the decreasing value of layer thickness will increase the number of layers needed to complete the fabrication process, results in increasing the time taken in fabricating the specimens. Moreover, layer thickness of the part also affects the surface roughness, in which the smaller the value of the layer thickness, the better the surface roughness is. This comparison can be seen in the figure below. From the figure, lower thickness layers give more accurate part produced, however, the time taken to finish a certain part is increasing due to the increasing of number of layers.

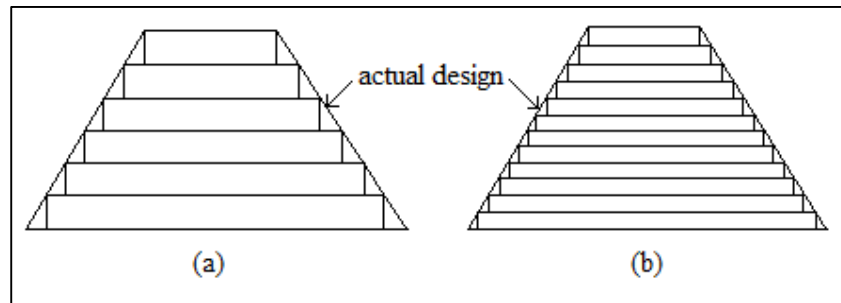


Figure 2.11: Effect of (a) Higher and (b) Lower Layer Thicknesses on Surface Roughness and Part Accuracy

There is a researcher experimenting with layer thickness on wind tunnel RP model. Daneshmand *et. al* created FDM model of a wing-body-tail launch vehicle configuration to be tested in the wind tunnel by applying various layer thicknesses of 0.178 mm, 0.254 mm, and 0.33 mm. They found that the FDM models did not have as smooth a finish as did the metal models, and they concluded that the layer thickness does have an effect on the aerodynamics characteristics in high Mach number speeds, where the effect is less drastic than at lower Mach numbers (S. Daneshmand, 2008).

Sood *et. al* experimented on layer thickness as one of the selected parameters, and they did a study on three responses, which are tensile, flexural, and impact strength. They concluded that high number of layers results in a high temperature gradient towards the bottom of the part, hence increase diffusion between adjacent raster and results in improved strength. However, high temperature gradient also causes distortion between layers. In the meantime, increase number of layers will increase the number of heating and cooling cycles. This condition will cause residual stress accumulation increases, hence distortion, interlayer cracking, and part delamination will be occurred, results in reduce strength (Anoop Kumar Sood, 2010).

CHAPTER III

METHODOLOGY

3.1 Charts

Within the time of completion of this project, it will be easy to complete with the aid of charts, in order to keep track with time for the whole project. In this section, two types of charts will be presented; they are Gantt chart, and flow chart.

3.1.1 Gantt Chart

The methodology of this project can be simplified using Gantt chart for better visualization. This chart keeps track with time for weekly progress of the whole project, and acts as the project planner. All the stages are clearly shown in the Gantt chart below to show the progress of this project until its completion.

Project Title: Investigation of Printing Parameters & Performance of Low Cost & Commercial FDM Printers

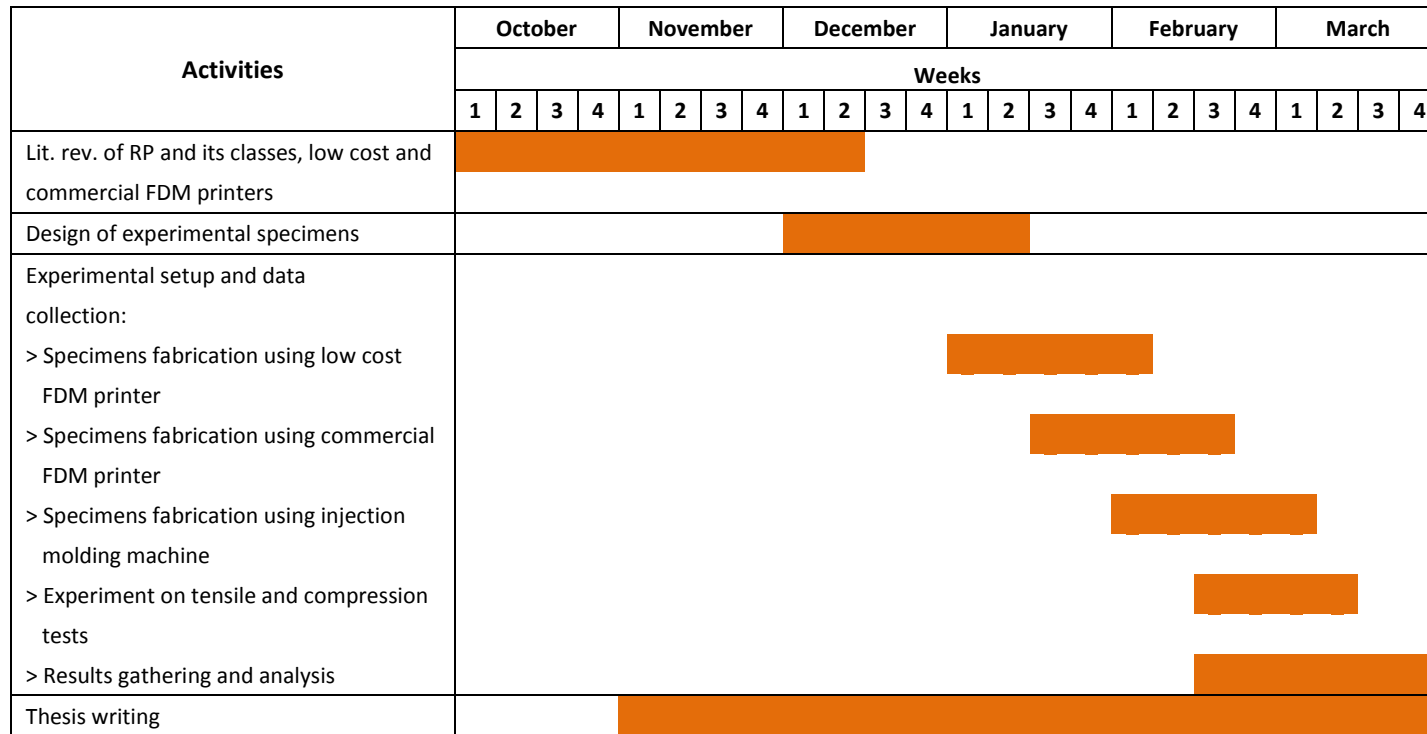


Figure 3.1: Project Gantt Chart

3.1.2 Flow Chart

In this section, the details for the progress will be shown step by step. In particular, the connection between each stage will be shown in a manner of consecutive processes. Some loops also are shown in order to depict the repetitive process for the particular stage. The flow chart can be summarized as in Figure 3.2 below.

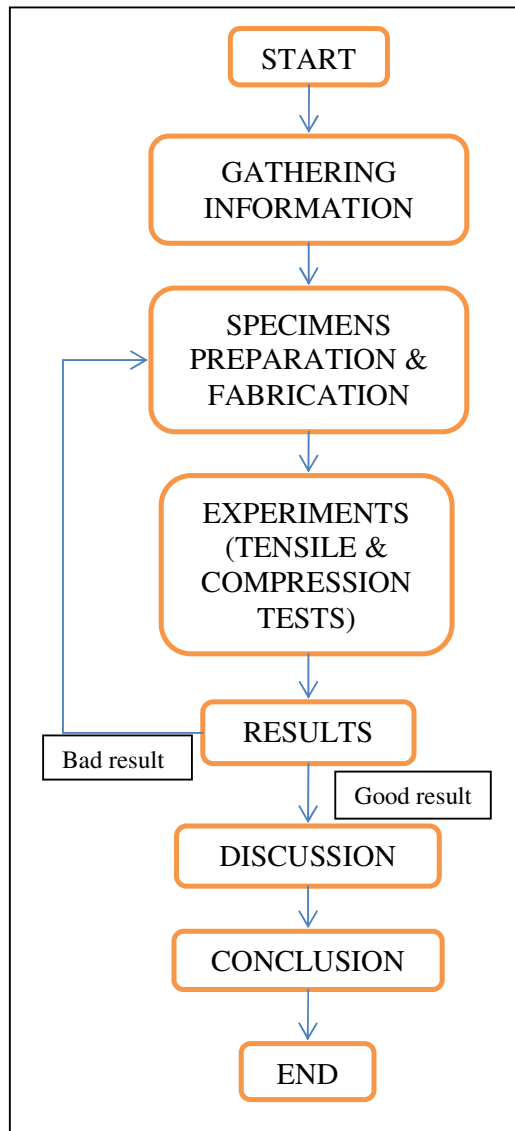


Figure 3.2: Project Flow Chart

Referring to the specimens' preparation and fabrication section in the flow chart above, this section also has its flow chart, in order to get a clear view of the things that should be done. In this section, the types of specimens are divided into three parts: specimens for tensile, compression, and torsional tests. The fabrication of specimens will be divided into two parts: specimens from the commercial FDM machine, and specimens from the low-cost FDM machine. Figure 3.3 below shows the detail of the process.

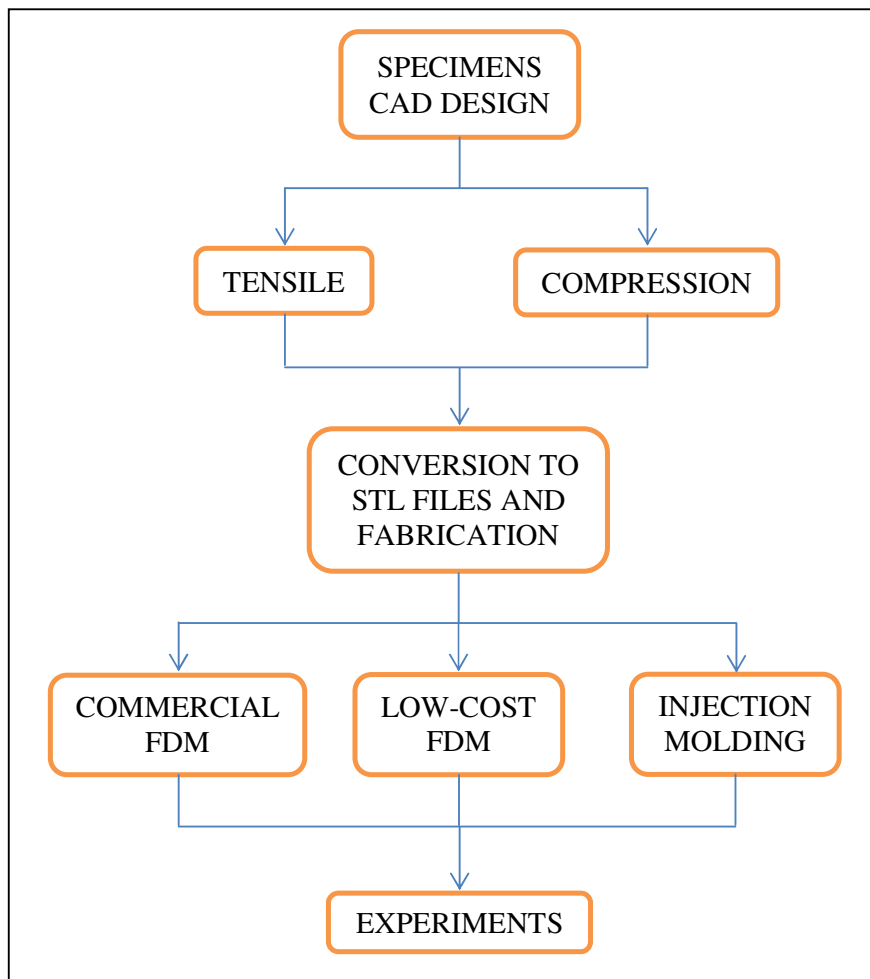


Figure 3.3: Specimens Fabrication and Preparation Flow Chart

3.2 Information Gathering

Based on previous research work from various researchers, the results they obtained are gathered. This is important in order to validate this research work, and to check if this research work is acceptable or vice versa. At this stage, several types of specimens can be found, with several factors to be experimented.

3.3 Experimental Setup

In this section, there are three steps taken within the completion of this project. The specimens were prepared based on the previous research studies. Once the specimens needed are prepared, they were fabricated by using both low-cost and commercial FDM. There are three specimens fabricated for each case in this project. Experiments of tensile and compression tests were conducted in order to determine the ultimate tensile and compressive stresses from each case.

3.3.1 Specimens Preparation

After gathering relevant information within the research scope, several experimental runs will be conducted. In this research, several specimens will be prepared with different types of process parameters. The process parameters that will be taken into consideration layer thickness and infill material percentage.

The geometry of the specimens will be based on ASTM D638 type V standard for the tensile specimens. The dimensions of the specimens that will be applied in this project is 63.5 mm for the length and 9.53 mm for the width in a dogbone shape with 9.53 mm in length and 3.18 mm in width at the narrow part, with a loading rate of 1mm/min for tensile test; and 25.4 mm in height with 12.7 mm width and length for compression test according to ASTM D695, with a loading rate of 2 mm/min. These

specimens will be drawn and converted into STL files. There are several software can be used to draw the specimens. ProE software will be used to draw all the specimens. Shown below are the specimens for tensile, and compression tests together with their dimensions in mm.

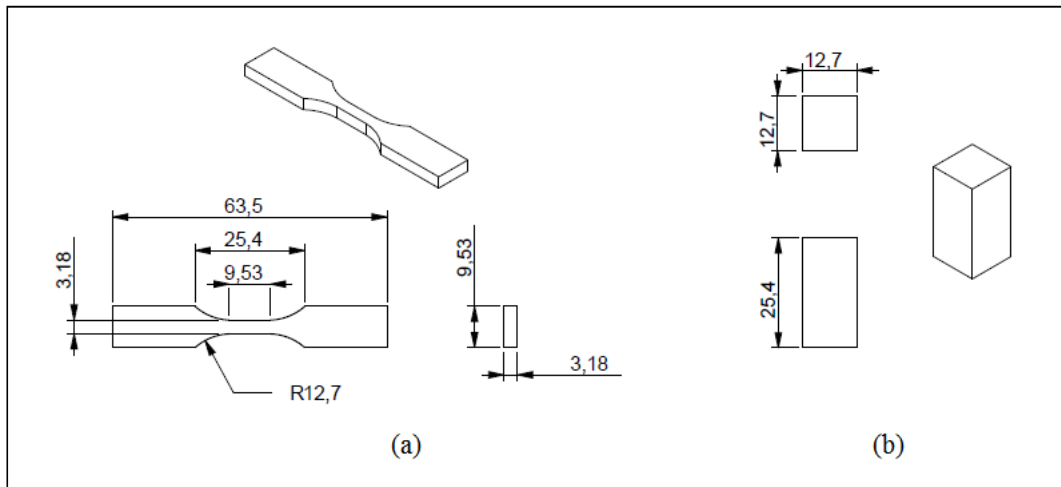


Figure 3.4: Dimensions of Specimens of (a) Tensile Test, and (b) Compression Test

After the files converted into STL extension files, they will be imported into software used for operating the FDM machine. In the software, the file will be sliced to G-code according to the parameters set, and prediction fabrication time will be displayed. Software used for the commercial FDM is called CatalystEX version 4.3. Generally, the x, y, and z-axes are shown in the box where the specimen will be placed, as shown in the figure below. From the figure, there are properties of the specimen that can be set before start the fabrication process.

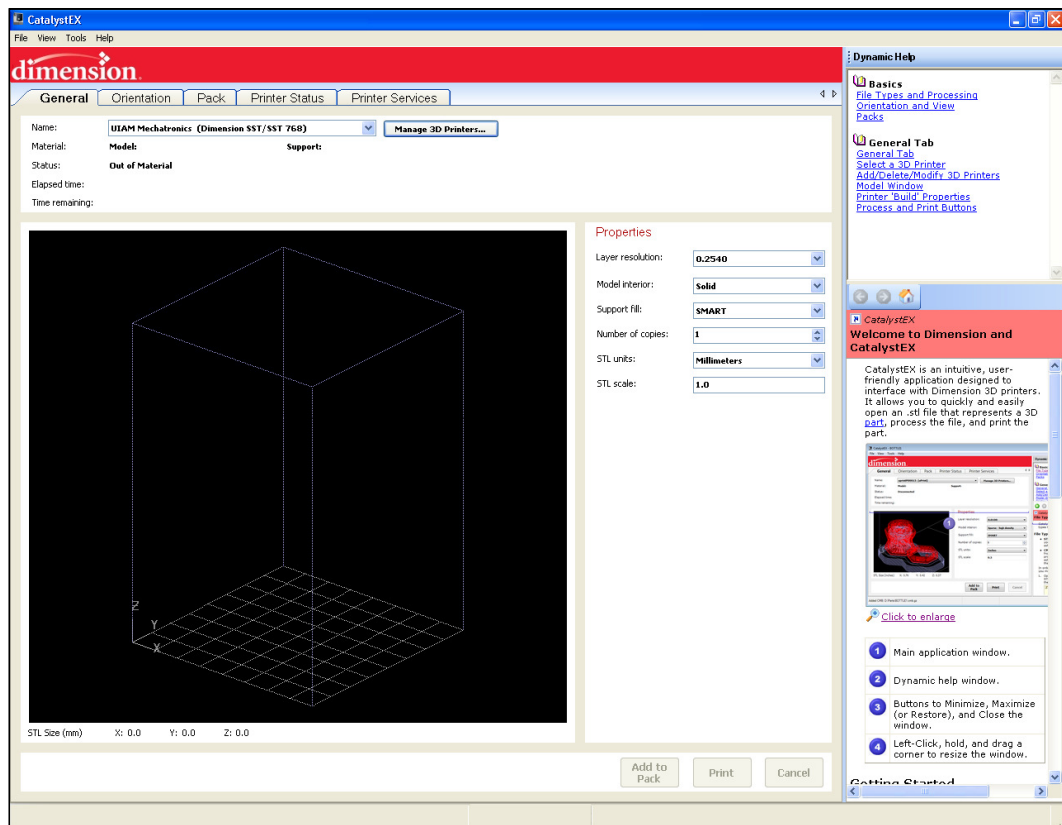


Figure 3.5: CatalystEX 4.3 Software Interface

For the low-cost FDM printer, software named Cura will be used. The software version is Cura 12.08, as shown in the figure below. The x, y, and z-axes are clearly shown in the figure. After an STL file loaded into the software, the estimated filament volume, print time, and cost that will be involved in the specimen fabrication will occur at the left bottom corner of the software interface.

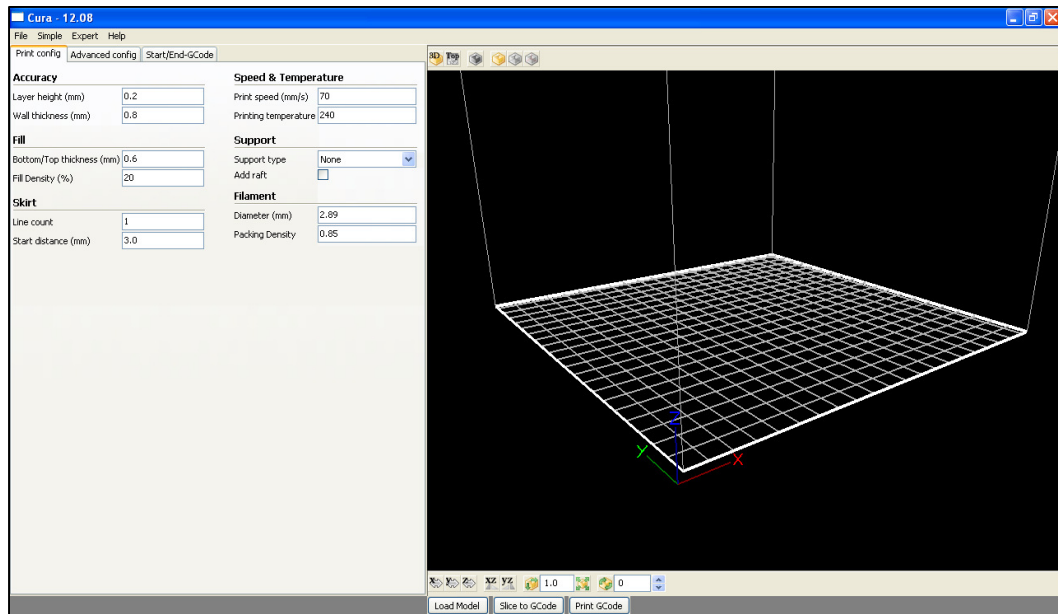


Figure 3.6: Cura 12.08 Software Interface

3.3.2 Specimens Fabrication

Specimens will be fabricated by using two types of FDM machines, commercial and low-cost printer. The commercial FDM machine used is Dimension SST 768, while low-cost FDM printer used is called Ultimaker as shown below.

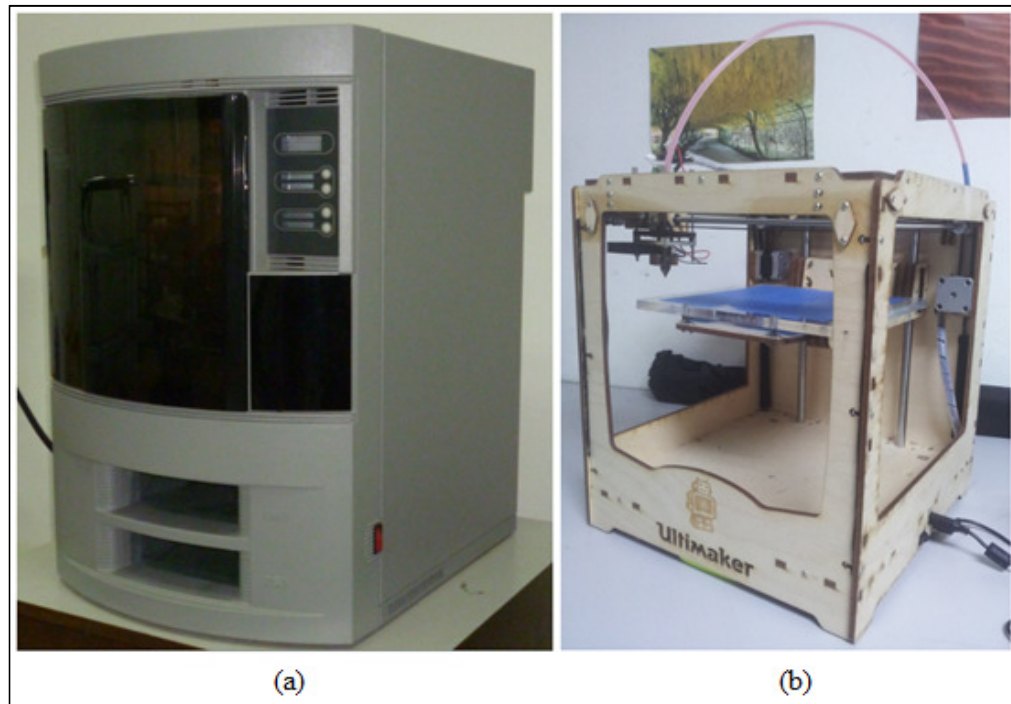


Figure 3.7: (a) Dimension SST 768 and (b) Ultimaker FDM Machines

In order to validate the upcoming results, some specimens will be fabricated by using the plastic injection molding as a benchmark result. The model of the injection molding machine used for this project is BOY 22M. This is vital to validate whether the results are acceptable or vice versa. The machine can be seen in the figure below.



Figure 3.8: Plastic Injection Molding Machine

Several parameters will be considered in preparing the specimens. Based on the study, the parameters that will be taken into consideration in this research are layer thickness, and infill percentage. For this research, two types of layer thickness will be applied, which are 0.2540 mm, and 0.3302 mm. 45/-45° orientation will be used as the default setting. Infill percentage will be applied in this research are 50%, and 100%. Both settings for the layer thickness and the infill material percentage are chosen due to the limitation on the CatalystEX version 4.3 software, where those are the only settings available. Air gap will be neglected and set to be negative gap as proven to be stronger and denser than zero air gap by Sung-Hoon *et. al.* Shown below are (a) the fabrication process, (b) the ready specimen for compression, and (c) the ready specimen for tensile by using Ultimaker printer.

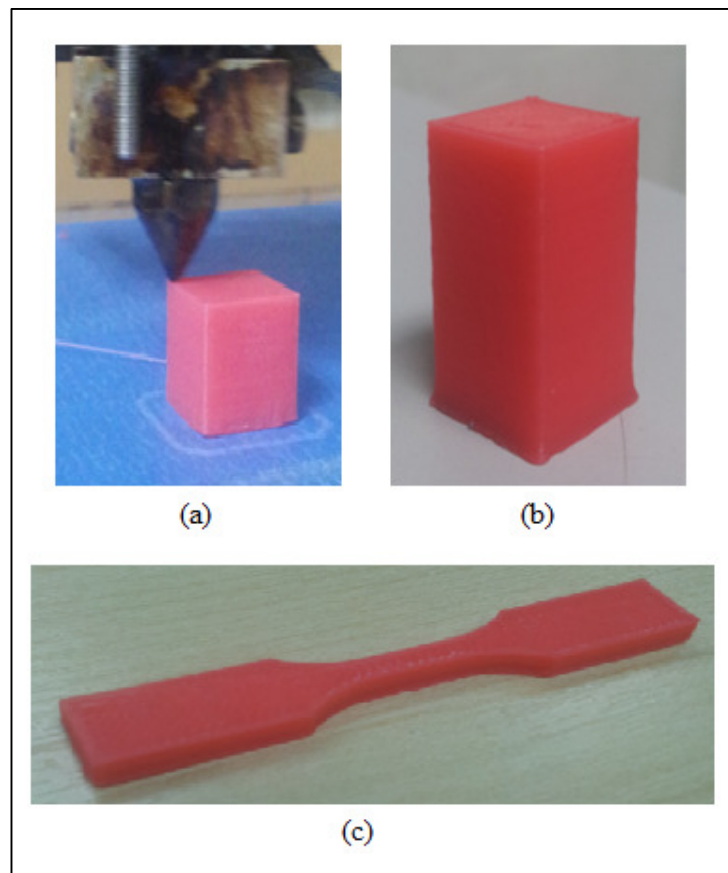


Figure 3.9: (a) Fabrication Process, (b) Compression, and (c) Tensile Ready Specimen

3.3.3 Experiments

After fabricating the specimens, experiment such as tensile test, and compression test will be conducted. At least three readings will be measured for each specimen, and an average result will be determined. The results obtained will be compared between specimens fabricated by commercial and low-cost FDM printers, with specimen fabricated by injection molding as a benchmark result. Tensile test and compression test will be made using the same machine, which is INSTRON 3369 testing machine with a maximum load of 50 kN, as shown below.



Figure 3.10: INSTRON 3369 Testing Machine

CHAPTER IV

RESULTS

In this project, the main objective is to determine the reliability of the low-cost FDM machine in parts fabrication, and comparing both low-cost and commercial FDM machines with the specimens fabricated using an injection molding process, as a benchmark result. In this section, several cases will be outlined, with the respective results. Each specimen for each test will be undergoing three tests, and an average result will be determined. The results shown in this section are the average results for each case. The results for each specimen in all cases will be shown in the Appendix section.

4.1 Tensile Test

Several specimens with different parameters will be tested. In this section, the specimens that will be tested are using the common shape of tensile specimen, which is called dogbone shape. The dimension of the specimens is according to the ASTM D638 type V standard, which is 63.5 mm in length, 9.53 mm in width, and 3.18 mm thickness, and the dimension at the testing area is 9.53 mm in length, and 3.18 mm in width. This dimension is applied to all tensile test specimens. The infill percentage of the specimens will be varies from 50% and 100% for 0.2540 mm and 0.3302 mm layer thicknesses.

According to the standard, the suitable tensile rate should be applied is 5 mm/min. However, for this test, the tensile rate applied is 1 mm/min, due to the small size of the specimens used. Shown below are the failure mode of tensile test for both commercial and low-cost FDM specimens.

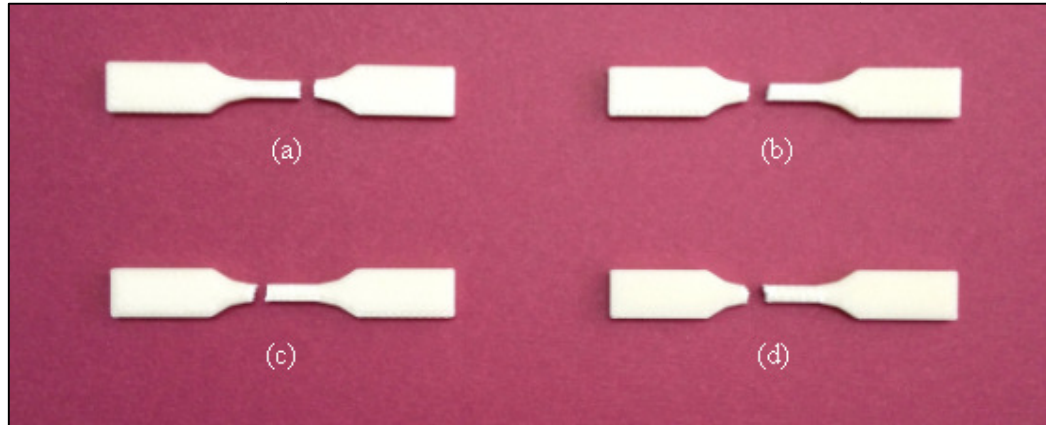


Figure 4.1: Commercial FDM Specimens' Failure Mode: (a) Case 1; (b) Case 2; (c) Case 3; and (d) Case 4

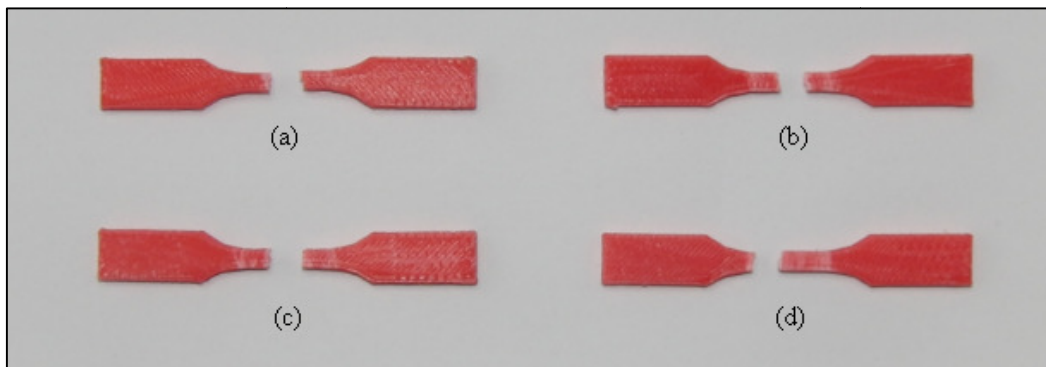


Figure 4.2: Low-Cost FDM Specimens' Failure Mode: (a) Case 1; (b) Case 2; (c) Case 3; and (d) Case 4

4.1.1 Case 1 (0.3302mm, 50%)

In the first case for tensile test, the specimens are having 0.3302mm layer thickness, with infill material percentage of 50%. These parameters are applied in the specimens for both commercial and low-cost FDM machines. The experiments were done three times in order to get the average result for both types of machines, and a

graph of the average readings was plotted showing the comparison in terms of ultimate tensile stress, as shown in Figure 4.3 below.

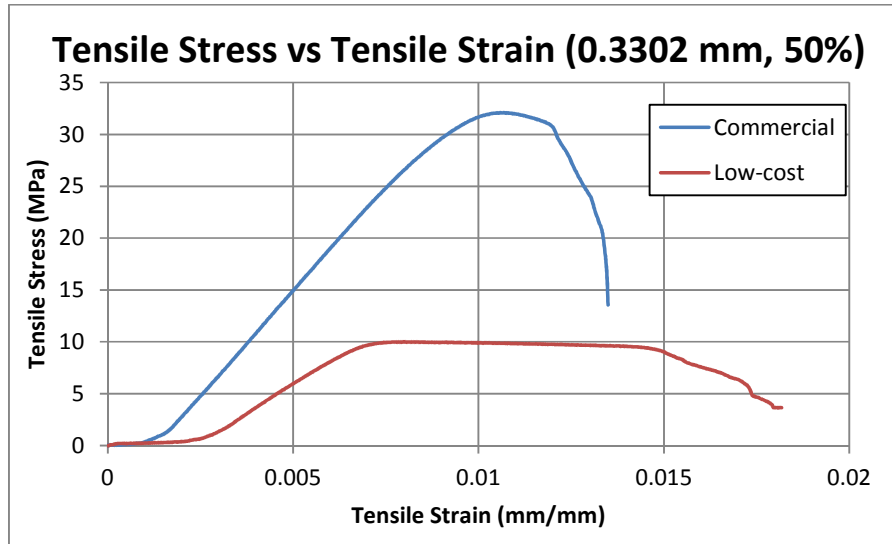


Figure 4.3: Graph of Tensile Comparison of Stress-Strain for Case 1

From the graph above in Figure 4.3, the achievable average tensile stress by the 3specimen fabricated using commercial FDM is 32.1463 MPa, meanwhile the low-cost fabricated specimens achieved 10.18369 MPa. This is probably because of the uneven interlayer atomic bonding of the low-cost FDM machine, due to the open cavity at the sides of the machine itself, which results in the environment effect such as the rapid temperature drop of the specimens during the fabrication process. The other results regarding the test were constructed in Table 4.1.

Table 4.1: Case 1 Tensile Test Average Results for Commercial and Low-Cost FDMs

Specimen	Maximum Load (N)	Ultimate Tensile Stress (MPa)	Tensile Extension at Ultimate Tensile Stress (mm)	Strain at Ultimate Tensile Stress (mm/mm)
Commercial	325.0762	32.14630	0.680667	0.010719
Low-Cost	102.9815	10.18369	0.54231	0.008540

The results in Table 4.1 above were recorded during the tensile test experiment. The highest maximum load achieved before the specimens break was 325.0762 N and 102.9815 N for both commercial and low-cost FDM machines respectively. At the ultimate tensile stress achieved, the tensile extension recorded was 0.680667 mm and 0.54231 mm for both commercial and low-cost FDM machines respectively. Lastly for the strain recorded at ultimate tensile stress was 0.010719 mm/mm for commercial FDM and 0.008540 mm/mm for low-cost FDM.

4.1.2 Case 2 (0.3302mm, 100%)

Specimens used in case 2 were having a layer thickness of 0.3302 mm, same as case 1, but the infill material percentage is 100%. Both commercial and low-cost FDM machines were used these parameters during the fabrication process. Overall there were three specimens fabricated and tested, and the average reading was calculated. The graph of tensile test average results was plotted in order to show the tensile stress comparison between commercial and low-cost FDM machines.

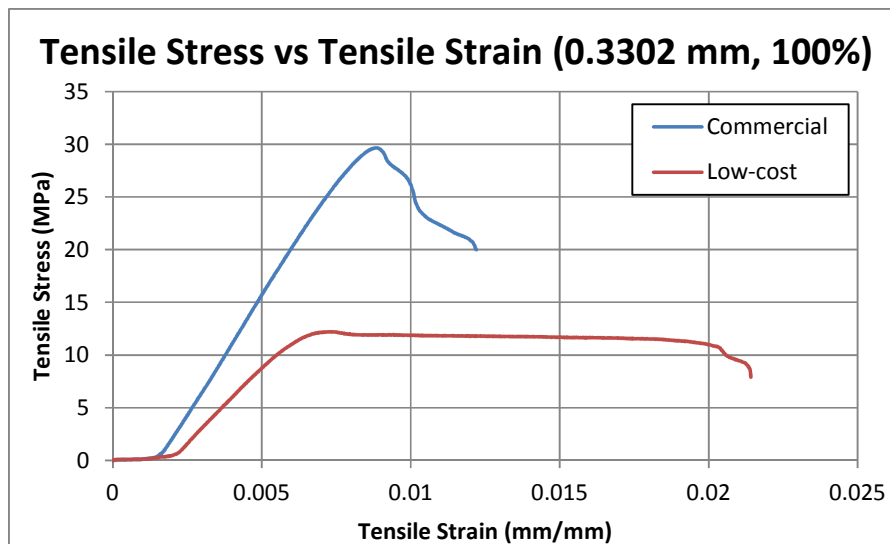


Figure 4.4: Graph of Tensile Comparison of Stress-Strain for Case 2

As shown in the graph in Figure 4.4 above, the pattern variation between the two machines is quite large. It shows that the commercial FDM specimens achieved the

ultimate tensile stress of 30.259 MPa, and the low-cost FDM achieved 12.66995 MPa. From the graph, it can be seen that the low-cost FDM specimens were having high resistance from the tensile strain reading of about 0.0064 mm/mm to near 0.02 mm/mm during the experiment before they completely broke. The other results recorded during the experiment were constructed in Table 4.2 below.

Table 4.2: Case 2 Tensile Test Average Results for Commercial and Low-Cost FDMs

Specimen	Maximum Load (N)	Ultimate Tensile Stress (MPa)	Tensile Extension at Ultimate Tensile Stress (mm)	Strain at Ultimate Tensile Stress (mm/mm)
Commercial	305.7575	30.2590	0.588521	0.009268
Low-Cost	128.1236	12.66995	0.56614	0.008916

From the table above, the commercial FDM machine was having a maximum load of 305.7575 N, while the low-cost FDM machine was recorded at only 128.1236 N, which is about 41.9% of the value of the commercial FDM recorded. During the ultimate tensile stress state of the specimens, the commercial FDM was having 0.588521 mm tensile extension, and the low-cost was recorded at 0.56641 mm, in which the results for both were almost identical. Lastly, the commercial FDM was having the strain of 0.009268 mm/mm and the low-cost FDM was having 0.008916 mm/mm strain recorded at ultimate tensile stress.

4.1.3 Case 3 (0.2540mm, 50%)

The layer thickness applied for the specimens in case 3 was 0.2540 mm, with 50% infill material percentage. Another three specimens were fabricated for both commercial and low-cost FDM machines, in order to get the average results respectively. After the experiment finished, all three results for each machine will be gathered and the average result will be calculated. Shown below is the comparison between the two FDM machines for their average results.

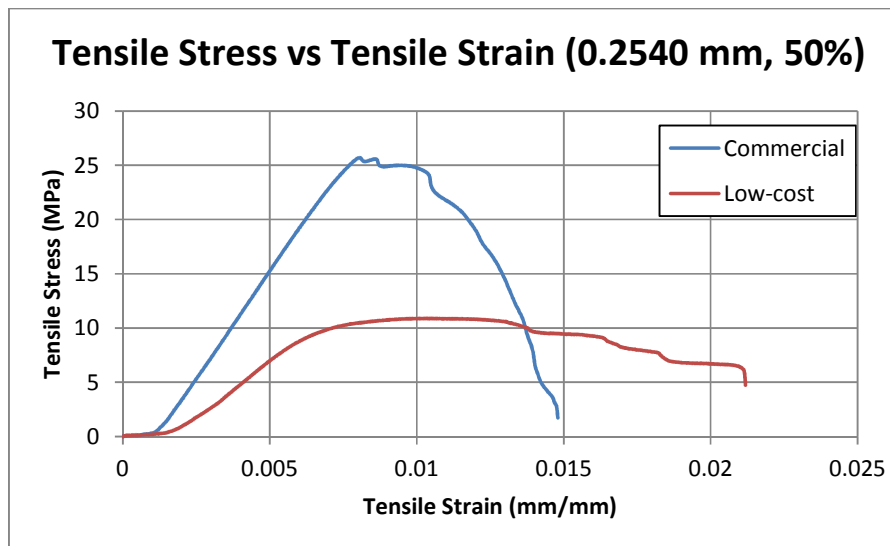


Figure 4.5: Graph of Tensile Comparison of Stress-Strain for Case 3

As shown in Figure 4.5 above, once again the specimens fabricated by the commercial FDM was having higher ultimate tensile stress of 26.92973 MPa, and low-cost FDM specimens were having an average of 10.92310 MPa. There are also other results obtained, and were tabulated in Table 4.3 below.

Table 4.3: Case 3 Tensile Test Average Results for Commercial and Low-Cost FDMs

Specimen	Maximum Load (N)	Ultimate Tensile Stress (MPa)	Tensile Extension at Ultimate Tensile Stress (mm)	Strain at Ultimate Tensile Stress (mm/mm)
Commercial	272.3243	26.92973	0.556292	0.008760
Low-Cost	110.4587	10.92310	0.61402	0.009670

Based on Table 4.3 above, the comparison between the commercial and low-cost FDM machines can be seen clearly. The maximum load obtained for commercial FDM was 272.3243 N and for low-cost FDM was 110.4587 N. The percentage difference for the low-cost FDM to commercial FDM in terms of maximum load is 40.56% and in terms of ultimate tensile stress is also 40.56%. However, the low-cost FDM machine was recorded to have 0.61402 mm tensile extension at the ultimate tensile stress,

compared to 0.556292 mm tensile extension recorded from the commercial FDM, which is slightly lower. This shows that the specimens fabricated using low-cost FDM can extend a bit longer than the specimens fabricated using commercial FDM before reaching the ultimate tensile stress state. Because of that, the strain recorded for the low-cost FDM fabricated specimens was 0.009670 mm/mm, compared to 0.008760 mm/mm of the strain recorded for the commercial FDM fabricated specimens, as seen in the graph in Figure 4.5.

4.1.4 Case 4 (0.2540mm, 100%)

The final specimens for tensile test were having the layer thickness of 0.2540 mm but with 100% infill material percentage for both commercial and low-cost FDM machines. Same as in previous cases, three specimens for each machine were fabricated and tested. Once the experiment finished, the average result for both machines were calculated, and a graph was plotted out of it. The graph can be seen below in Figure 4.6.

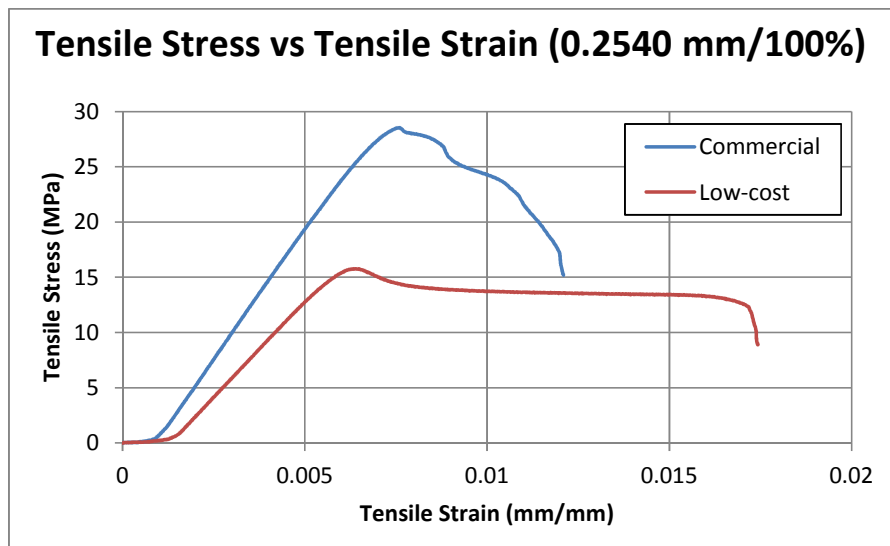


Figure 4.6: Graph of Tensile Comparison of Stress-Strain for Case 4

Based on the graph above, the comparison of the performance between the commercial and low-cost FDM machines can be seen clearly. The achievable ultimate tensile stress for both commercial and low-cost FDM machines was 28.89397 MPa and

15.80230 MPa respectively. From the average results for both machines, the low-cost FDM was 54.69% compared to the commercial FDM. Other results were also obtained and tabulated in Table 4.4 below.

Table 4.4: Case 4 Tensile Test Average Results for Commercial and Low-Cost FDMs

Specimen	Maximum Load (N)	Ultimate Tensile Stress (MPa)	Tensile Extension at Ultimate Tensile Stress (mm)	Strain at Ultimate Tensile Stress (mm/mm)
Commercial	292.1772	28.89297	0.50352	0.007929
Low-Cost	159.7991	15.80230	0.405687	0.006389

The other results that were obtained after the experiment finished were maximum load, tensile extension and strain at ultimate tensile stress. Since the commercial FDM recorded higher ultimate tensile stress, the maximum load recorded also was high, which is 292.1772 N, compared to the low-cost FDM result which is 159.7991 N. The result obtained from the low-cost FDM is about 54.69% from the commercial FDM machine. The tensile extension recorded for both commercial and low-cost FDM was 0.50358 mm and 0.405687 mm respectively. Lastly, the strain recorded at ultimate tensile strain was 0.007929 mm/mm for the commercial FDM and 0.006389 mm/mm for the low-cost FDM.

4.1.5 Plastic Injection Molding

Another three specimens were fabricated by using plastic injection molding machine. After the experiment finished, the specimens broke into cup-and-cone formation. This formation can be seen in Figure 4.7 below.

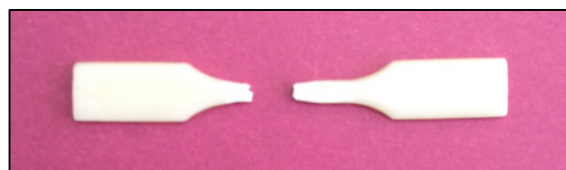


Figure 4.7: Plastic Injection Molding Specimen's Failure Mode

The intention of conducting three experiments is to get an average result. This result obtained is only for benchmark purpose, as a measurement for the results obtained from commercial and low-cost FDM machines. The graph of the average result for the plastic injection molding specimens is plotted as shown below.

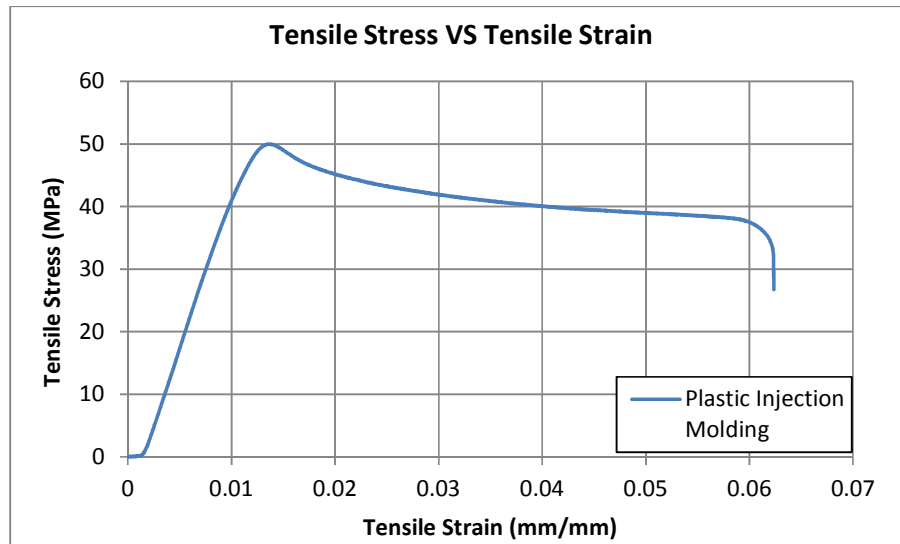


Figure 4.8: Graph of Stress-Strain for Plastic Injection Molding

As seen in the graph above, the ultimate tensile stress obtained is really high, which is 50.19363 MPa. This is due to the mechanism of the mold, in which the atom of the plastic particles was bonded very tightly and uniformly before it cools down. The homogeneity results in the high mechanical strength for the specimens. The other results were also obtained and tabulated in Table 4.5 as seen below.

Table 4.5: Tensile Test Average Results for Plastic Injection Molding Specimens

Specimen	Maximum Load (N)	Ultimate Tensile Stress (MPa)	Tensile Extension at Ultimate Tensile Stress (mm)	Strain at Ultimate Tensile Stress (mm/mm)
PIM	507.5781	50.19363	0.862791	0.013587

Based on the table above, the maximum load recorded for the specimens fabricated by the plastic injection molding was 507.5781 N, due to the high strength

bonding of the plastic particles. During the experiment, the tensile extension achieved was 0.862791 mm and the strain was 0.013587 mm/mm at ultimate tensile stress.

4.1.6 Results Comparison between FDM Machines and Injection Molding

In this section, a comparison of the results obtained was made between commercial FDM, low-cost FDM, and injection molding specimens. The results obtained were shown in a bar chart of the ultimate tensile stress achieved for all cases.

This chart was constructed as shown below in Figure 4.9.

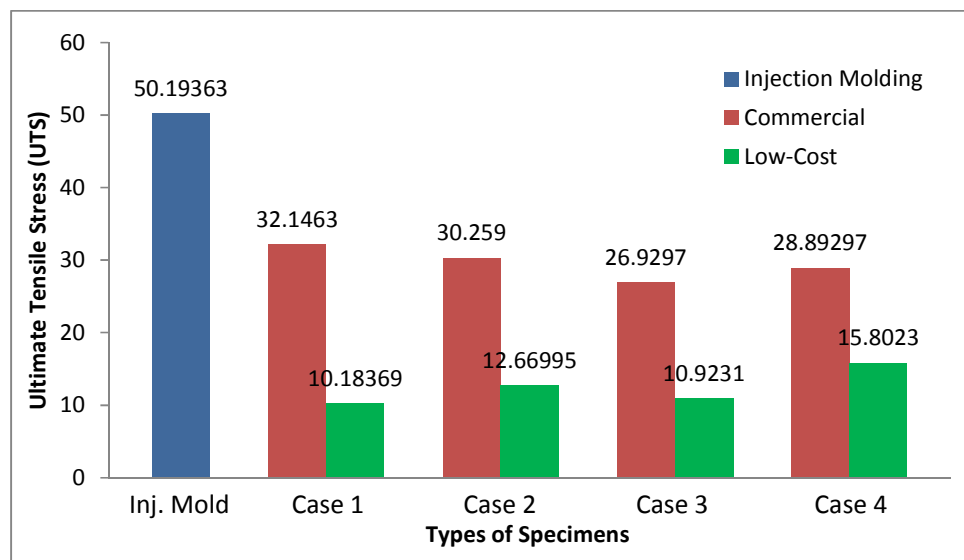


Figure 4.9: Ultimate Tensile Stresses Comparison between FDM Machines and Injection Molding

Referred to the bar chart above, the ultimate tensile stress achieved by the specimens fabricated using injection molding is 50.19363 MPa. As observed, the results obtained from the specimens fabricated using the commercial FDM machine are ranged around 53.65% to 64.04% from the injection molding result. Meanwhile for the low-cost FDM machine, the results obtained are ranged from 20.28% to 31.48% from the injection molding result. In order to compare the results between the two FDM machines based on the bar chart as well, the percentage of tensile stress of the low-cost FDM to the commercial FDM machine is ranged from 31.68% to 54.69%. However, for

the low-cost FDM machine, the layer thickness seems to affect the tensile stress of the specimen, which means, in order to get higher tensile stress, the parts fabricated using the low-cost FDM machine must use lower layer thickness setting.

4.2 Compression Test

Same with tensile test specimens, the specimens for compression test also will be varied in terms of the infill percentage of 50%, and 100%, as well as the layer thickness of 0.2540 mm, and 0.3302 mm. It has a square shape with a dimension of 25.4 mm in height, and 12.7 mm in length and width, which is based on ASTM D695 standard. The compression rate applied is 2 mm/min. The effect of compression test on the specimens might vary between buckling, shearing, double barreling, barreling, homogeneous compression, and compressive instability due to work-softening material depending on the length over diameter ratio (L/D) (M. Altenaiji, 2012). All the specimens' failure modes can be seen as shown in Figure 4.10 and Figure 4.11 below.

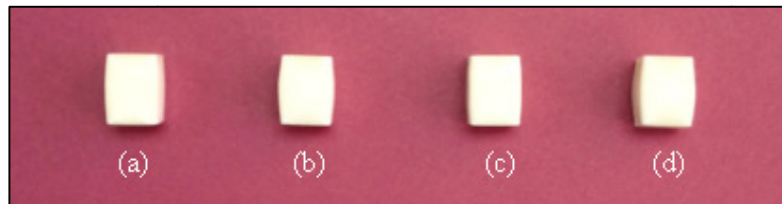


Figure 4.10: Commercial FDM Specimens' Failure Mode: (a) Case 1; (b) Case 2; (c) Case 3; and (d) Case 4

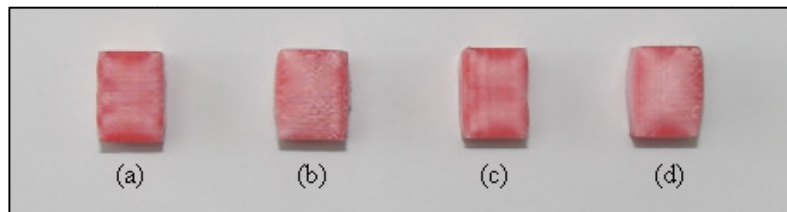


Figure 4.11: Low-Cost FDM Specimens' Failure Mode: (a) Case 1; (b) Case 2; (c) Case 3; and (d) Case 4

4.2.1 Case 1 (0.3302mm, 50%)

For the first case of compression test, the parameters used for the specimens were similar with the first case of tensile test. The layer thickness of the specimens was 0.3302 mm and the infill material percentage was 50%. Three specimens for each FDM were fabricated and experimented thoroughly. After the tests finished, an average result for each FDM was calculated, and a graph of comparison between those two FDM machines was plotted, as shown in Figure 4.12 below.

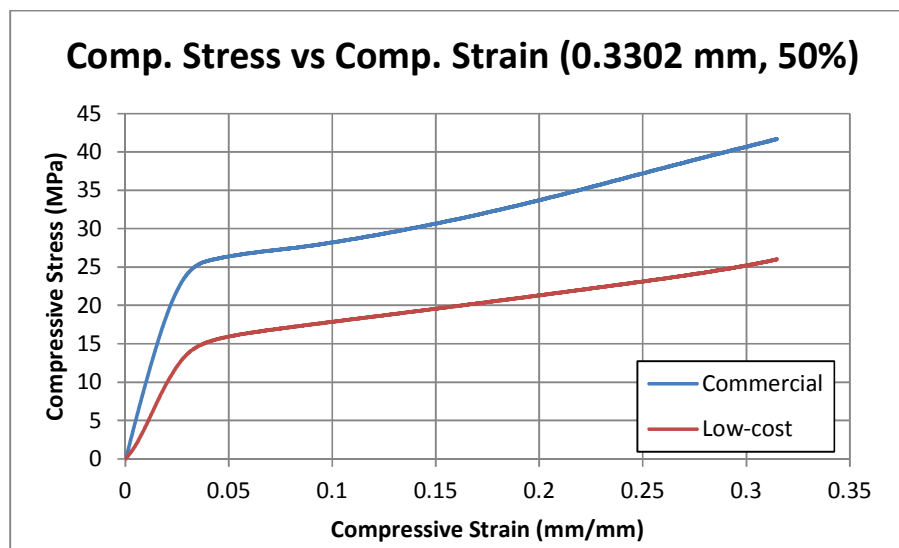


Figure 4.12: Graph of Compression Comparison of Stress-Strain for Case 1

Referring to the graph above, both specimens were kept increasing after reaching the elastic deformation stage. After the specimens reached about 8 mm compressive extension, the experiment was stopped. It was achieved an ultimate compressive stress of 25.60 MPa for the commercial FDM and 15.48 MPa for the low-cost FDM. The percentage of the low-cost FDM result compared to the commercial FDM is 60.49%. Other results obtained were tabulated in a table as shown in Table 4.6 as follow.

Table 4.6: Case 1 Compression Test Average Results for Commercial and Low-Cost FDMs

Specimen	Maximum Load (kN)	Ultimate Compressive Stress (MPa)	Comp. Extension at Maximum Comp. Load (mm)	Strain at Ultimate Comp. Stress (mm/mm)
Commercial	6.721	25.60	0.95773	0.037706
Low-Cost	4.197	15.48	0.99544	0.039190

Based on the table above, the commercial FDM recorded the maximum load of 6.721 kN instead of 4.197 kN recorded for the low-cost FDM. During the specimens achieved the ultimate compressive stress, the compression extension recorded were 0.95773 mm and 0.99544 mm for both commercial and low-cost FDM respectively. Lastly, the values of strain recorded for both commercial and low-cost FDM recorded during the ultimate compressive stress were 0.037706 mm/mm and 0.039190 mm/mm respectively.

4.2.2 Case 2 (0.3302mm, 100%)

Layer thickness of 0.3302 mm and infill material percentage of 100% was applied to the specimens in case 2 for both commercial and low-cost FDM machines. Another three specimens were fabricated for both commercial and low-cost FDM machines. After the experiments finished, an average result for both machines was calculated. A graph containing both average results was plotted in order to show the comparison between those two machines. The graph mentioned is shown in Figure 4.13 below.

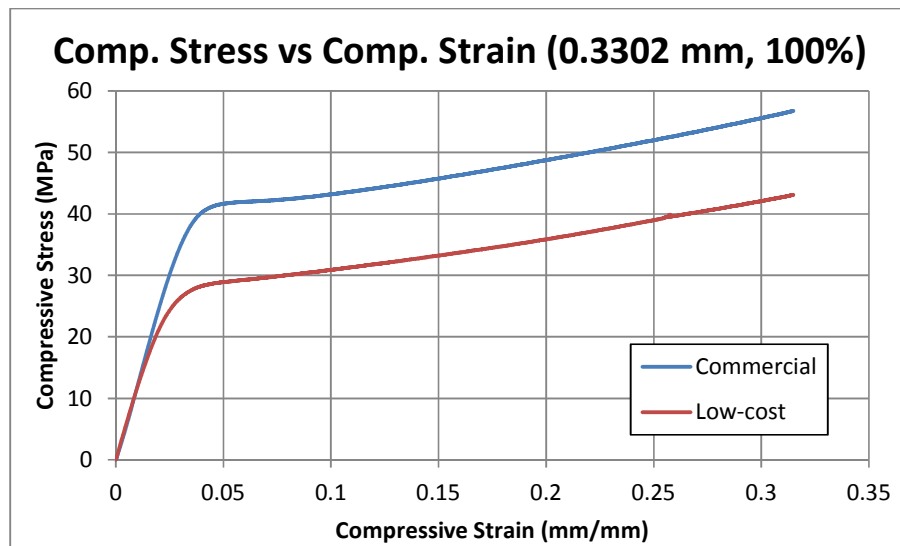


Figure 4.13: Graph of Compression Comparison of Stress-Strain for Case 2

Referring to the graph above, the pattern increment after reaching the elastic deformation is identical, only the value is different. For the commercial FDM, the ultimate compressive stress achieved was 41.16 MPa, and for the low-cost FDM was 28.21 MPa when the experiment was stopped after reaching the extension of about 8 mm. In terms of percentage, the low-cost FDM reached 68.54% from the commercial FDM result. The other results obtained were recorded in a table as shown in Table 4.7 below.

Table 4.7: Case 2 Compression Test Average Results for Commercial and Low-Cost FDMs

Specimen	Maximum Load (kN)	Ultimate Compressive Stress (MPa)	Comp. Extension at Maximum Comp. Load (mm)	Strain at Ultimate Comp. Stress (mm/mm)
Commercial	9.204	41.16	1.13463	0.044670
Low-Cost	6.987	28.21	0.90765	0.035734

The other results obtained were maximum load and strain at ultimate compressive stress. The maximum load for both commercial and low-cost FDM machines were 9.204 kN and 6.987 kN respectively. Having the compressive extension of 1.13463 mm during the ultimate compressive stress was the commercial FDM, the

value of strain obtained was 0.044670 mm/mm. For the low-cost FDM, the compressive extension during the ultimate compressive stress was 0.90765 mm, and the strain value recorded was 0.035734 mm/mm.

4.2.3 Case 3 (0.2540mm, 50%)

In case 3, the layer thickness applied was 0.2540 mm and the infill material percentage was 50%. Three specimens were fabricated for both FDM machines. When the experiment finished, an average result was calculated for both FDM machines. Then, a graph consists of both results was plotted in order to show the comparison between the two machines. The graph can be seen in Figure 4.14 below.

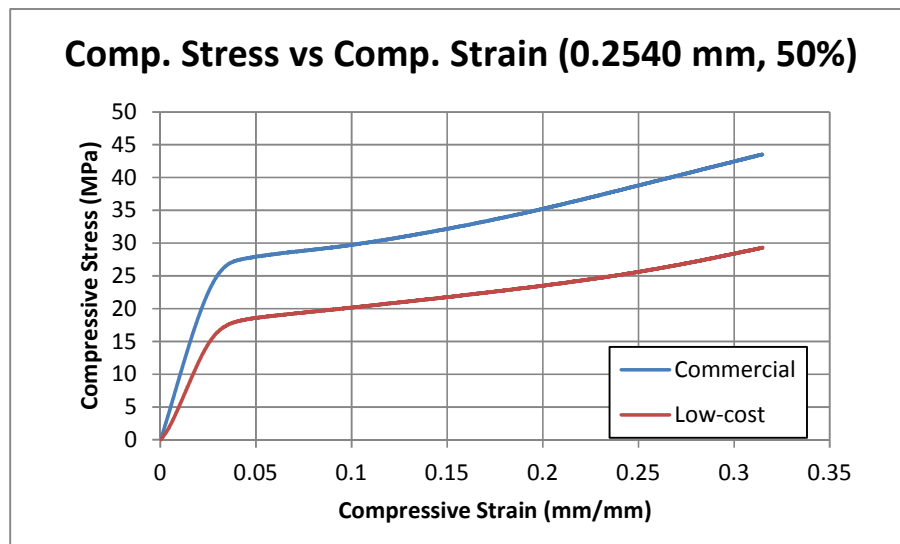


Figure 4.14: Graph of Compression Comparison of Stress-Strain for Case 3

Based on the graph above, the ultimate compressive stress for both commercial and low-cost FDM machines recorded was 27.25 MPa and 17.98 MPa respectively. The experiment was stopped whenever the compressive extension is about to reach 8 mm, in which the final height of the specimens were about 2/3 from its original height. The low-cost FDM was reached about 65.98% from the commercial FDM. The other results such as maximum load and strain were also obtained and tabulated in Table 4.8 below.

Table 4.8: Case 3 Compression Test Average Results for Commercial and Low-Cost FDMs

Specimen	Maximum Load (kN)	Ultimate Compressive Stress (MPa)	Comp. Extension at Maximum Comp. Load (mm)	Strain at Ultimate Comp. Stress (mm/mm)
Commercial	7.026	27.25	0.98654	0.038840
Low-Cost	4.765	17.98	0.99656	0.039235

Referring to the table above, the maximum load recorded for the commercial FDM was 7.026 kN and for the low-cost FDM was 4.765 kN. During the ultimate compressive stress, the compressive extension for both commercial and low-cost FDM machines was 0.98654 mm and 0.99656 mm respectively. The value of strain recorded for both FDM machines was 0.038840 mm/mm and 0.039235 mm/mm respectively.

4.2.4 Case 4 (0.2540mm, 100%)

The final experiment for the compression test was using the specimens with the same layer thickness of 0.2540 mm, but the infill material percentage was 100%. Another three specimens were fabricated for each FDM machine. These specimens were then experimented in order to get the average result. Once tested, the average results were obtained, they then were plotted into a graph for comparison purpose. This graph can be seen in Figure 4.15 below.

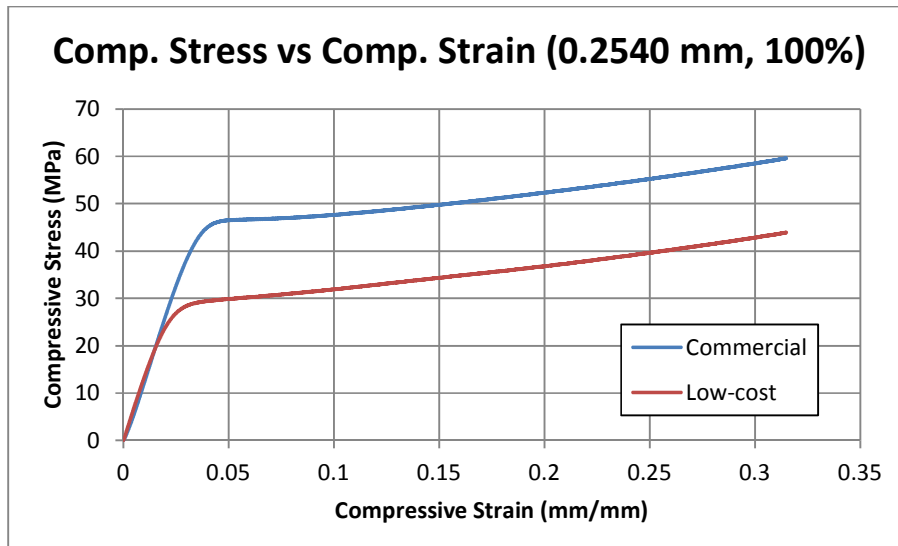


Figure 4.15: Graph of Compression Comparison of Stress-Strain for Case 4

Based on the graph above, the patterns for both specimens were almost identical, except on the value of the ultimate compressive stress. The commercial FDM machine recorded 46.17 MPa for the ultimate compressive stress, while the low-cost FDM machine recorded 29.03 MPa. In percentage, the low-cost FDM reached 62.88% from the commercial FDM. Shown below in Table 4.9 is the other results obtained during the experiment.

Table 4.9: Case 4 Compression Test Average Results for Commercial and Low-Cost FDMs

Specimen	Maximum Load (kN)	Ultimate Compressive Stress (MPa)	Comp. Extension at Maximum Comp. Load (mm)	Strain at Ultimate Comp. Stress (mm/mm)
Commercial	9.613	46.17	1.15008	0.045279
Low-Cost	7.093	29.03	0.87659	0.034511

Based on the table above, the commercial FDM was recorded to have a maximum load of 9.613 kN, compared to the low-cost FDM with 7.093 kN maximum load recorded. When the specimens reached the ultimate compressive stress, the compressive extension recorded were 1.15008 mm for the commercial FDM and 0.87659 mm for the low-cost FDM. Lastly, the commercial FDM was recorded to have

the strain value of 0.045279 mm/mm, while the low-cost FDM was recorded to have the strain value of 0.034511 mm/mm.

4.2.5 Results Comparison between FDM Machines

The results obtained for both commercial and low-cost FDM machines will be compared in this section. The intention is to justify the reliability of the low-cost FDM machine compared to the commercial FDM. The results obtained were shown in a bar chart of the ultimate compressive stress achieved in all cases. This chart was constructed and shown in Figure 4.16 below.

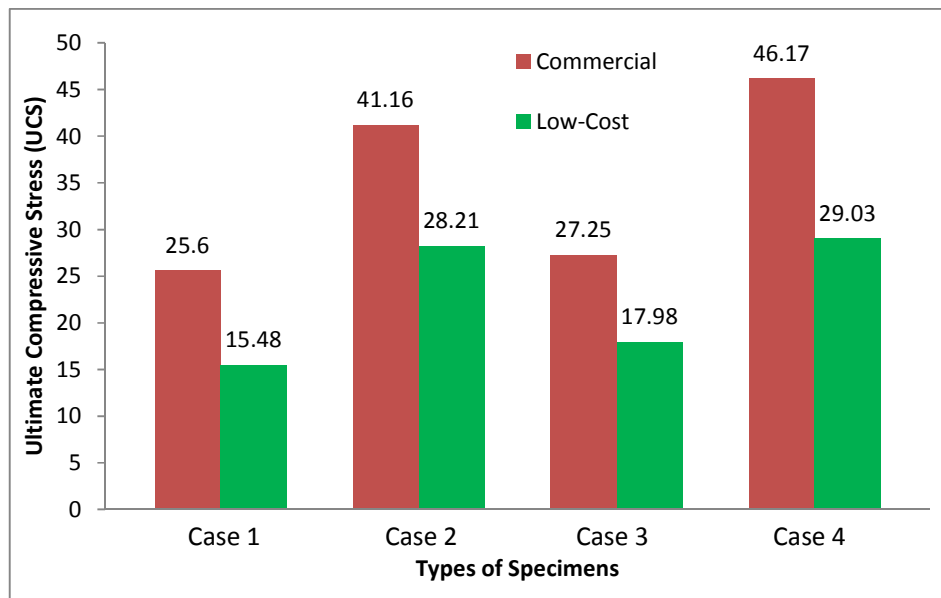


Figure 4.16: Ultimate Compressive Stresses Comparison between FDM Machines

Based on the bar chart above in Figure 4.16, it shows the comparison for all ultimate compressive stresses for all specimens fabricated by using commercial and low-cost FDM machines. In case 1, the highest possible ultimate compressive stress for commercial FDM was recorded at 25.60 MPa, meanwhile for low-cost FDM was recorded at 15.48 MPa. In case 2, the commercial FDM achieved was 41.16 MPa ultimate compressive stress, and low-cost FDM was recorded at 28.21 MPa. This variation between case 1 and case 2 was caused by the infill material percentage of 50%

and 100% respectively. Same thing goes to case 3 and case 4, where the variation of the results was caused by the infill material percentage. In case 3, the commercial FDM was achieved the ultimate compressive stress of 27.25 MPa, while the low-cost FDM was recorded at 17.98 MPa. Lastly in case 4, the ultimate compressive stress recorded for the commercial FDM was 46.17 MPa, and 29.03 MPa recorded for the low-cost FDM.

From the chart above, commercial FDM is still dominating in terms of achievable compressive stress for all cases. By calculation, the low-cost FDM machine achieved between 60.49% to 69.54% from the commercial FDM machine.

CHAPTER V

DISCUSSIONS

From all the results obtained, there are some discussions could be made throughout this project. Recall that the main objective of this project is to determine the reliability of the low-cost FDM machine in parts fabrication, and comparing both low-cost and commercial FDM machines with the specimens fabricated using an injection molding process, as a benchmark result. For this purpose, specimens for tensile and compression tests are made by using two types of FDM machine, commercial and low-cost. The low-cost FDM machine used in this project is called Ultimaker, meanwhile the commercial FDM machine used is Dimension SST 768. There are also specimens that fabricated by using the plastic injection molding method, which the machine is called BOY 22M, by using the same material. The intention is to get a benchmark result in order to compare the results obtained from the rapid prototyped specimens.

Basically, there are two parameters taken into consideration in this project. They are layer thickness, and infill material percentage. The layer thicknesses of the specimens applied are 0.2540 mm and 0.3302 mm, for each infill material percentage of 50%, and 100%. In order to get a more accurate result, three specimens were fabricated for each parameter set for tensile and compression, and then an average result is

calculated and tabulated in a table. Stress-strain graphs for tensile test and compression test were plotted for evaluation purpose.

5.1 Tensile Test

After a number of experiments were done for tensile test, all the results are tabulated in tables and stress-strain curves were created for each case, in which the detail results can be referred in the Appendices section. Overall, there are four cases done for tensile test using the commercial FDM and the low-cost FDM, and one case for the injection molding method for the benchmark result.

Based on the tensile test results shown in Figure 4.6, for the commercial FDM specimens with 100% infill material percentage, for the layer thickness of 0.3302 mm was achieved 30.259 MPa ultimate tensile stress, while the layer thickness of 0.2540 mm was achieved a lower ultimate tensile stress of 28.89297 MPa. This is because, higher layer thickness acquired a lower number of layers compared to the lower layer thickness for the same specimens, hence the distortion effect will be minimized and strength increases (Anoop Kumar Sood, 2010). From a previous research, the layer thickness of 0.3556 mm was found the most effective according to the S/N analysis (R. Anitha, 2001), which is nearer to the layer thickness of 0.3302 mm applied in this research.

However, the results obtained from the low-cost FDM machine seems not agreed with the results of the commercial FDM. They were inverted from the commercial FDM, where the smaller layer thickness achieved higher ultimate tensile stress. This situation occurred probably due to the open cavity of the low-cost FDM machine, hence the temperature of the specimen was disturbed by the environment, and affecting the mechanical properties.

While comparing the infill material percentage results obtained within the same layer thickness, it is found that the 50% infill material percentage can be applied in fabricating parts that not required any or small amount of force or strength, such as headphone holder, cell phone stand, and name plate. From the results obtained from the low-cost FDM machine, it was recorded that for the layer thickness of 0.3302 mm, the percentage difference of 50% with 100% infill material percentage was 80.38%, while for the layer thickness of 0.2540 mm, the percentage difference was 69.12%. Based on the percentage, the low-cost FDM can be used for fabricating parts with 50% infill material percentage, hence the time consumed will be shortened, and the material usage can be minimized. This situation is similar to the commercial FDM, the percentage difference between 50% and 100% infill material percentage within the same layer thickness is about 93.21%, hence it is suitable to use the machine in fabricating parts by using only 50% infill material percentage, as it will save the time consumed and material usage. In order to compare from both commercial and low-cost FDM machines, the low-cost FDM should be considered more as it has a low initial cost for the machine (Evan Malone, 2007).

However, when it comes to the parts that need to be used under a certain strength or force, the commercial FDM machine should be considered if the strength needed is more than 15.8023 MPa, based on the results obtained from the low-cost FDM machine with the parameters of 0.2540 mm layer thickness and 100% infill material percentage. This is because, that is the limitation of the strength of the low-cost FDM machine as obtained from the experiment. Below than that, the low-cost FDM machine is still a reliable machine in fabricating small parts or specimens.

5.2 Compression Test

Same thing goes to compression test, where all results were obtained and calculated from their average values. In this section, results obtained from previous chapter will be elaborated. The results obtained consist of commercial and low-cost FDM machines. In total, there were four cases for both commercial and low-cost FDM machines. An average result was obtained for each case.

The results obtained for compression test were acceptable, as compared for case 4 result of the commercial FDM which was 46.17 MPa and the low-cost FDM which was 29.03 MPa, with a result obtained by a previous researcher where the ultimate compressive stress of commercial FDM was about 36.47 MPa (C. S. Lee, 2007). There was a big difference between the result obtained in this project of 46.17 MPa with their result of 36.47 MPa due to the unspecified layer thickness applied in their experiment, even though the raster angle applied was the same of 45°/-45°.

According to the experiment by another researcher, the ultimate compressive stress obtained from their experiment was about 33 MPa (Sung-Hoon Ahn, 2002). The raster angle applied in their research was the same with this experiment. However, the layer thickness was different, as they applied the layer thickness of 0.003 inches (0.0762 mm). As seen from the results of the commercial FDM in this experiment, case 2 (0.3302 mm layer thickness, 100% infill material percentage) obtained the ultimate compressive stress of 41.16 MPa, and case 4 (0.2540 mm layer thickness, 100% infill material percentage) obtained 46.17 MPa. As a comparison between these two results, higher number of layers was resulting in the higher ultimate compressive stress, however, an increasing number of layers also can caused strength of the part (Anoop Kumar Sood, 2010).

Based on the results obtained, the patterns of the ultimate compressive stress for both commercial and low-cost FDM machines were identical according to their respective parameter sets. From the specimens of 0.3302 mm layer thickness of the commercial FDM machine, the percentage difference obtained in terms of ultimate compressive stress of 50% to 100% infill material percentage is 62.20%, while the low-cost FDM machine recorded a difference of 54.87%, while specimens of 0.2540 mm layer thickness were recorded at the percentage difference of 59.02% and 61.94% respectively for the commercial and the low-cost FDM machines, in terms of ultimate compressive stress of 50% to 100% infill material percentage.

Based on the percentage calculated for the low-cost FDM, the infill material percentage of 100% should be considered in order to fabricate parts, so that it will long lasting. This is because for 50% infill material obtained almost half strength compared to the 100% infill material. As compared between the layer thickness, 0.3302 mm layer thickness can be considered in making parts, since it achieved about 97.18% from the 100% infill material, results in lesser material usage and hence saving cost.

CHAPTER V

CONCLUSIONS

6.1 Conclusions

Throughout the whole project, there are some conclusions can be made as the outputs. Based on the discussions made in the previous chapter, it can be said that the low-cost FDM printer is also reliable in terms of fabricating small parts, and is comparable with the commercial FDM. However, there are some problems with these two FDM printers when compared with the specimens fabricated with injection molding, where the strength obtained from tensile test is much higher than that with these two FDM printers fabricated specimens.

From the tensile test results, the low-cost FDM machine achieved 31.68% to 54.69% of the ultimate tensile test from the results of the commercial FDM machine obtained. This percentage varies due to the effect of the density of the specimens. However, this percentage also can be increased by using a smaller layer thickness when operating the low-cost FDM machine. In terms of compression test results, the low-cost FDM machine achieved 62.44% to 75.56% from the commercial FDM machine results. This percentage shows that the low-cost FDM machine is remarkably reliable in fabricating small parts.

Above all, the low-cost FDM printer can be concluded as reliable in making small parts, but the following parameters should be taken into consideration:

- a) Small layer thickness of the part.
- b) Orientation of $45^{\circ}/-45^{\circ}$.
- c) Negative air gap between adjacent layer in the same layer.
- d) 100% infill material for a stronger bond between material atoms.

6.2 Future Works

As for the future work, specimen of the compression should be fabricated using plastic injection molding machine. Then the specimen can be tested for compression test, hence can be made as the benchmark result for validation of the FDM specimen results obtain in this project.

Other than that, different parameters can be considered other than the two parameters considered in this research, which are layer thickness and infill material percentage. Parameters such as layer orientation, and build direction can be taken into consideration in the future research work.

Besides tensile and compression test, several tests such as 3-point bending test, torsional test, and Charpy impact test also can be conducted in order to validate the mechanical properties of the specimen fabricated using the low-cost and commercial FDM machines.

REFERENCES

- A.W. Fatimatuzahraa, B. F., W.A.Y Yusoff. (2011). The effect of employing different raster orientations on the mechanical properties and microstructure of Fused Deposition Modeling parts. *IEEE Symposium*, 22 - 27.
- Abbas Azari, S. N. (2009). The evolution of rapid prototyping in dentistry: a review. *Rapid Prototyping Journal*, 15(3), 216 - 225.
- Anoop Kumar Sood, R. K. O., S. S. Mahapatra. (2010). Parametric appraisal of mechanical property of fused deposition modelling processed parts. *Materials and Design*, 31, 287 - 295.
- Arnilotta, A. (2006). Assessment of surface quality on textured FDM prototypes. *Rapid Prototyping Journal*, 12(1), 35 - 41.
- B. Wiedemann, H.-A. J. (1999). Strategies and applications for rapid product and process development in Daimler-Benz AG. *Computers in Industry*, 39, 11–25.
- Bruker. Tribology and Mechanical Testing Unit. In Bruker (Ed.), *Test Method for Measuring the Shore Hardness of Soft Materials Using the CETR-UMT 2 or CETR-APEX per ASTM D2240-00*.
- C. S. Lee, S. G. K., H. J. Kim, S. H. Ahn. (2007). Measurement of anisotropic compressive strength of rapid prototyping parts. *Journal of Materials Processing Technology*, 187 - 188, 627 - 630.
- Chua Chee Kai, L. K. F., Lim Chu-Sing. (2010). *Rapid Prototyping: Principles and Applications* (3rd ed.): World Scientific Publishing Co. Pte. Ltd.

- Cooper, K. G. (2001). *Rapid Prototyping Technology: Selection and Application*: Marcel Dekker Inc.
- David Espalin, K. A., David Rodrigues, Francisco Medina, Matthew Posner, Ryan Wicker. (2010). Fused deposition modelling of patient-specific polymethylmethacrylate implants. *Rapid Prototyping Journal*, 16(3).
- Dimension. 1200es 3D Printer Series Retrieved 10th September 2012, from <http://www.dimensionprinting.com/3d-printers/printing-productspecs1200series.aspx%5C>
- Dimension. Elite 3D Printer Retrieved 10th September 2012, from <http://www.dimensionprinting.com/3d-printers/printing-productspecs-elite.aspx>
- Evan Malone, H. L. (2007). Fab@Home: the personal desktop fabricator kit. *Rapid Prototyping Journal*, 13(4), 245 - 255.
- Giorgio Colombo, S. F., Caterina Rizzi, Federico Rotini. (2010). A new design paradigm for the development of custom-fit soft sockets for lower limb prostheses. *Computers in Industry*, 61, 513–523.
- Hilbertcurve. Retrieved 10th September 2012, from http://en.wikipedia.org/wiki/Hilbert_curve
- J. Czyżewski, P. B., K. Gawęł, J. Meisner. (2009). Rapid prototyping of electrically conductive components using 3D printing technology. *Materials Processing Technology*(209), 5281–5285.
- Jacobs, P. F. (1992). *Rapid Prototyping & Manufacturing: Fundamentals of StereoLithography* (1st ed.): Society of Manufacturing Engineers.
- M. Altenaiji, G. K. S., & Y.Y. Zhao. (2012). Characterisation of Aluminium Matrix Syntactic Foams Under Static and Dynamic Loading. In N. Hu (Ed.), *Composites and Their Properties*: InTech.

Math-PlanePath Gallery. Retrieved 10th September 2012, from <http://user42.tuxfamily.org/math-planepath/gallery.html>

Noorani, R. I. (2006). *Rapid Prototyping: Principles and Applications*. New Jersey: John Wiley & Sons, Inc.

O. S. Es-Said, J. F., R. Noorani, M. Mendelson, R. Marloth, & B. A. Pregger. (2000). Effect of layer orientation on mechanical properties of rapid prototyped samples. *Material & Manufacturing Process*, 15(1), 107 – 122.

P. Rochusa, J.-Y. P., M. Van Elsen, J.-P. Kruth, R. Carrus, T. Dormal. (2007). New Applications of Rapid Prototyping and Rapid Manufacturing (RP/RM) Technologies for Space Instrumentation. *Acta Astronautica*, 61, 352 – 359.

Q. Sun, G. M. R., C.T. Bellehumeur, P. Gu. (2008). Effect of processing conditions on the bonding quality of FDM polymer filaments. *Rapid Prototyping Journal*, 14(2), 72 - 80.

R. Anitha, S. A., & P. Radhakrishnan. (2001). Critical parameters influencing the quality of prototypes in fused deposition modelling. *Journal of Materials Processing Technology*, 118, 385 - 388.

R.A. Buswell, R. C. S., A.G.F. Gibb, A. Thorpe. (2007). Freeform Construction: Mega-scale Rapid Manufacturing for construction. *Automation in Construction*, 16, 224–231.

S. Daneshmand, R. A., C. Aghanajafi. (2008). The Effect of Layer Thickness on Aerodynamic Characteristics of Wind Tunnel RP Models. *Journal of Fluid Science and Technology*, 3(1), 22 - 30.

S. Lohfeld, P. M., D. Serban, D. Boyle, G. O'Donnell, N. Peckitt. (2007). Engineering Assisted SurgeryTM: A route for digital design and manufacturing of customised maxillofacial implants. *Journal of Materials Processing Technology*, 183, 333–338.

- Singh, R. (2012). Some investigations for small sized product fabrication with FDM for plastic components. *Rapid Prototyping Journal*, 19(1).
- Suman Das, S. J. H., Colleen Flanagan, Adebisi Adewunmi, Karlin Bark, Cindy Chen, Krishnan Ramaswamy, Daniel Rose, Erwin Widjaja. (2003). Freeform fabrication of Nylon-6 tissue engineering scaffolds. *Rapid Prototyping Journal*, 9(1), 43 - 49.
- Sung-Hoon Ahn, M. M., Dan Odell, Shad Roundy, Paul K. Wright. (2002). Anisotropic material properties of fused deposition modelling ABS. *Rapid Prototyping Journal*, 8(4), 248 – 257.
- Y.G. Im, B. H. C., S.H. Seo, J.H. Son, S.I. Chung, H.D. Jeong. (2007). Functional prototype development of multi-layer board (MLB) using rapid prototyping technology. *Journal of Materials Processing Technology*, 187–188, 619–622.
- Zhang Yu, L. H. (2009). Application of Rapid Prototyping Technology in Die Making of Diesel Engine. *TSINGHUA SCIENCE AND TECHNOLOGY*, 14, 127-131.

APPENDICES

APPENDIX A – Tables for Each Specimen with Average Values for All Cases.

1) Tensile Test

Table 1: Tensile Test Results for Case 1 for Commercial FDM

Specimen	Maximum Load (N)	Ultimate Tensile Stress (MPa)	Tensile Extension at Ultimate Tensile Stress (mm)	Strain at Ultimate Tensile Stress (mm/mm)
1	325.3089	32.16931	0.691687	0.010893
2	331.7881	32.81002	0.666812	0.010501
3	318.1317	31.45957	0.683500	0.010764
Average	325.0762	32.14630	0.680667	0.010719

Table 2: Tensile Test Results for Case 2 for Commercial FDM

Specimen	Maximum Load (N)	Ultimate Tensile Stress (MPa)	Tensile Extension at Ultimate Tensile Stress (mm)	Strain at Ultimate Tensile Stress (mm/mm)
1	311.6325	30.81687	0.606937	0.009558
2	295.7374	29.24502	0.545250	0.008587
3	309.9027	30.64581	0.613375	0.009659
Average	305.7575	30.2590	0.588521	0.009268

Table 3: Tensile Test Results for Case 3 for Commercial FDM

Specimen	Maximum Load (N)	Ultimate Tensile Stress (MPa)	Tensile Extension at Ultimate Tensile Stress (mm)	Strain at Ultimate Tensile Stress (mm/mm)
1	275.0081	27.19513	0.541875	0.008533
2	297.1402	29.38375	0.620187	0.009767
3	244.8245	24.21032	0.506813	0.007981
Average	272.3243	26.92973	0.556292	0.008760

Table 4: Tensile Test Results for Case 4 for Commercial FDM

Specimen	Maximum Load (N)	Ultimate Tensile Stress (MPa)	Tensile Extension at Ultimate Tensile Stress (mm)	Strain at Ultimate Tensile Stress (mm/mm)
1	299.4301	29.61020	0.50681	0.007981
2	277.4761	27.43920	0.47525	0.007484
3	299.6254	29.62951	0.52850	0.008323
Average	292.1772	28.89297	0.50352	0.007929

Table 5: Tensile Test Average Results for All Cases for Commercial FDM

Case	Maximum Load (N)	Ultimate Tensile Stress (MPa)	Tensile Extension at Ultimate Tensile Stress (mm)	Strain at Ultimate Tensile Stress (mm/mm)
1	325.0762	32.1463	0.680667	0.010719
2	305.7575	30.2590	0.588521	0.009268
3	272.3243	26.9297	0.556292	0.008760
4	292.1772	28.89297	0.503520	0.007929

Table 6: Tensile Test Results for Case 1 for Low-Cost FDM

Specimen	Maximum Load (N)	Ultimate Tensile Stress (MPa)	Tensile Extension at Ultimate Tensile Stress (mm)	Strain at Ultimate Tensile Stress (mm/mm)
1	108.2547	10.70515	0.63344	0.009975
2	102.6314	10.14907	0.46156	0.007269
3	98.0583	9.69684	0.53194	0.008377
Average	102.9815	10.18369	0.54231	0.008540

Table 7: Tensile Test Results for Case 2 for Low-Cost FDM

Specimen	Maximum Load (N)	Ultimate Tensile Stress (MPa)	Tensile Extension at Ultimate Tensile Stress (mm)	Strain at Ultimate Tensile Stress (mm/mm)
1	136.9101	13.53884	0.45331	0.007139
2	133.0570	13.15781	0.44506	0.007009
3	114.4036	11.31320	0.80006	0.012599
Average	128.1236	12.66995	0.56614	0.008916

Table 8: Tensile Test Results for Case 3 for Low-Cost FDM

Specimen	Maximum Load (N)	Ultimate Tensile Stress (MPa)	Tensile Extension at Ultimate Tensile Stress (mm)	Strain at Ultimate Tensile Stress (mm/mm)
1	118.1107	11.67979	0.67519	0.010633
2	104.5285	10.33667	0.57181	0.009005
3	108.7369	10.75283	0.59506	0.009371
Average	110.4587	10.92310	0.61402	0.009670

Table 9: Tensile Test Results for Case 4 for Low-Cost FDM

Specimen	Maximum Load (N)	Ultimate Tensile Stress (MPa)	Tensile Extension at Ultimate Tensile Stress (mm)	Strain at Ultimate Tensile Stress (mm/mm)
1	162.3773	16.05725	0.411875	0.006486
2	156.8588	15.51153	0.393375	0.006195
3	160.1613	15.83811	0.411812	0.006485
Average	159.7991	15.80230	0.405687	0.006389

Table 10: Tensile Test Average Results for All Cases for Low-Cost FDM

Case	Maximum Load (N)	Ultimate Tensile Stress (MPa)	Tensile Extension at Ultimate Tensile Stress (mm)	Strain at Ultimate Tensile Stress (mm/mm)
1	102.9815	10.18369	0.54231	0.008540
2	128.1236	12.66995	0.56614	0.008916
3	110.4587	10.92310	0.61402	0.009670
4	159.7991	15.80230	0.405687	0.006389

Table 11: Tensile Test Results for Plastic Injection Molding

Specimen	Maximum Load (N)	Ultimate Tensile Stress (MPa)	Tensile Extension at Ultimate Tensile Stress (mm)	Strain at Ultimate Tensile Stress (mm/mm)
1	504.2915	49.86863	0.844937	0.013306
2	507.0056	50.13702	0.835125	0.013152
3	511.4371	50.57524	0.908312	0.014304
Average	507.5781	50.19363	0.862791	0.013587

2) **Compression Test**

Table 12: Compression Test Results for Case 1 for Commercial FDM

Specimen	Maximum Load (kN)	Ultimate Compressive Strength (MPa)	Comp. Extension at Maximum Comp. Load (mm)	Strain at Ultimate Comp. Stress (mm/mm)
1	6.620	25.08	0.97156	0.038251
2	6.717	25.66	0.97156	0.038251
3	6.827	26.05	0.93006	0.036617
Average	6.721	25.60	0.95773	0.037706

Table 13: Compression Test Results for Case 2 for Commercial FDM

Specimen	Maximum Load (kN)	Ultimate Compressive Strength (MPa)	Comp. Extension at Maximum Comp. Load (mm)	Strain at Ultimate Comp. Stress (mm/mm)
1	9.195	41.54	1.13538	0.044700
2	9.322	41.87	1.12850	0.044429
3	9.096	40.08	1.14000	0.044882
Average	9.204	41.16	1.13463	0.044670

Table 14: Compression Test Results for Case 3 for Commercial FDM

Specimen	Maximum Load (kN)	Ultimate Compressive Strength (MPa)	Comp. Extension at Maximum Comp. Load (mm)	Strain at Ultimate Comp. Stress (mm/mm)
1	6.872	26.08	0.96294	0.037911
2	7.081	27.86	0.99831	0.039304
3	7.124	27.80	0.99838	0.039306
Average	7.026	27.25	0.98654	0.038840

Table 15: Compression Test Results for Case 4 for Commercial FDM

Specimen	Maximum Load (kN)	Ultimate Compressive Strength (MPa)	Comp. Extension at Maximum Comp. Load (mm)	Strain at Ultimate Comp. Stress (mm/mm)
1	9.591	46.12	1.17175	0.046132
2	9.637	46.21	1.15175	0.045344
3	9.611	46.18	1.12675	0.044360
Average	9.613	46.17	1.15008	0.045279

Table 16: Compression Test Average Results for All Cases for Commercial FDM

Case	Maximum Load (kN)	Ultimate Compressive Strength (MPa)	Comp. Extension at Maximum Comp. Load (mm)	Strain at Ultimate Comp. Stress (mm/mm)
1	6.721	25.60	0.95773	0.037706
2	9.204	41.16	1.13463	0.044670
3	7.026	27.25	0.98654	0.038840
4	9.613	46.17	1.15008	0.045279

Table 17: Compression Test Results for Case 1 for Low-Cost FDM

Specimen	Maximum Load (kN)	Ultimate Compressive Strength (MPa)	Comp. Extension at Maximum Comp. Load (mm)	Strain at Ultimate Comp. Stress (mm/mm)
1	4.188	15.79	0.94644	0.037261
2	4.320	15.86	1.04138	0.040999
3	4.082	14.80	0.99850	0.039311
Average	4.197	15.48	0.99544	0.039190

Table 18: Compression Test Results for Case 2 for Low-Cost FDM

Specimen	Maximum Load (kN)	Ultimate Compressive Strength (MPa)	Comp. Extension at Maximum Comp. Load (mm)	Strain at Ultimate Comp. Stress (mm/mm)
1	6.241	23.27	0.77163	0.030379
2	6.834	26.51	0.82150	0.032343
3	7.885	34.84	1.12981	0.044481
Average	6.987	28.21	0.90765	0.035734

Table 19: Compression Test Results for Case 3 for Low-Cost FDM

Specimen	Maximum Load (kN)	Ultimate Compressive Strength (MPa)	Comp. Extension at Maximum Comp. Load (mm)	Strain at Ultimate Comp. Stress (mm/mm)
1	4.801	18.20	0.93975	0.036998
2	4.733	18.65	0.99981	0.039363
3	4.762	17.09	1.05013	0.041344
Average	4.765	17.98	0.99656	0.039235

Table 20: Compression Test Results for Case 4 for Low-Cost FDM

Specimen	Maximum Load (kN)	Ultimate Compressive Strength (MPa)	Comp. Extension at Maximum Comp. Load (mm)	Strain at Ultimate Comp. Stress (mm/mm)
1	6.599	25.80	0.83163	0.032741
2	7.791	33.60	0.96650	0.038051
3	6.888	27.70	0.83163	0.032741
Average	7.093	29.03	0.87659	0.034511

Table 21: Compression Test Average Results for All Cases for Low-Cost FDM

Case	Maximum Load (kN)	Ultimate Compressive Strength (MPa)	Comp. Extension at Maximum Comp. Load (mm)	Strain at Ultimate Comp. Stress (mm/mm)
1	4.197	15.48	0.99544	0.039190
2	6.987	28.21	0.90765	0.035734
3	4.765	17.98	0.99656	0.039235
4	7.093	29.03	0.87659	0.034511

APPENDIX B – Graphs for Each Specimen for All Cases.

1) Tensile Test

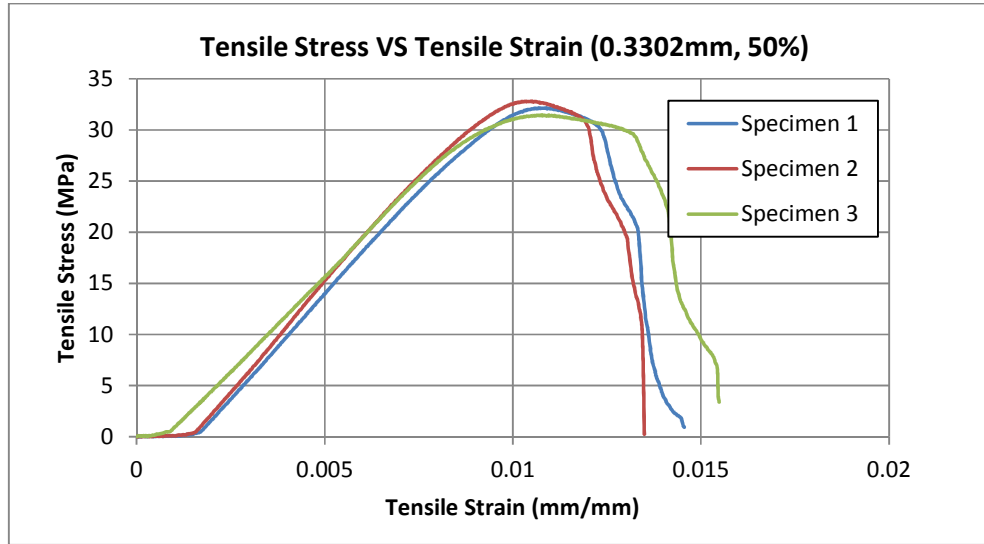


Figure 1: Tensile Stress - Strain Graph for Case 1 for Commercial FDM

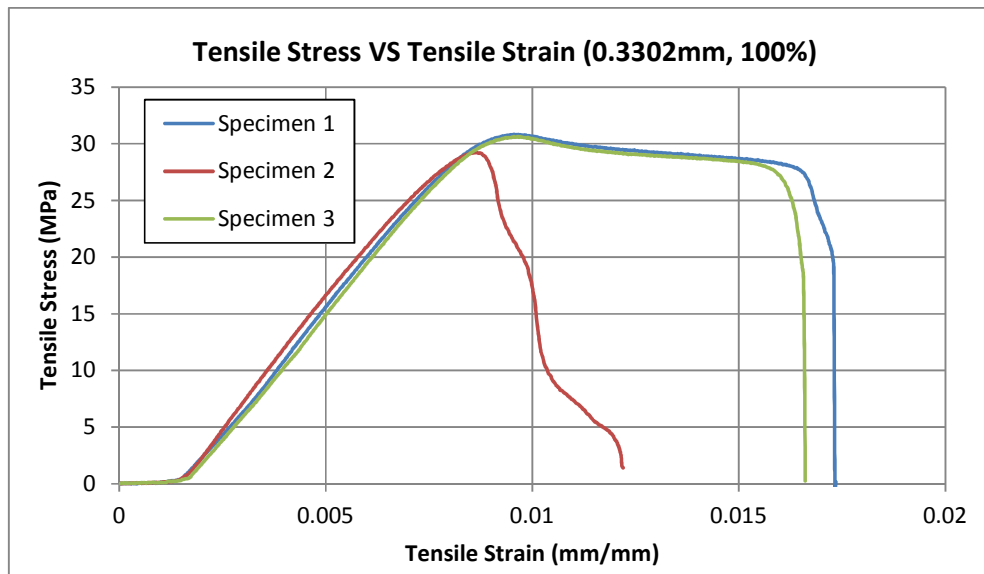


Figure 2: Tensile Stress - Strain Graph for Case 2 for Commercial FDM

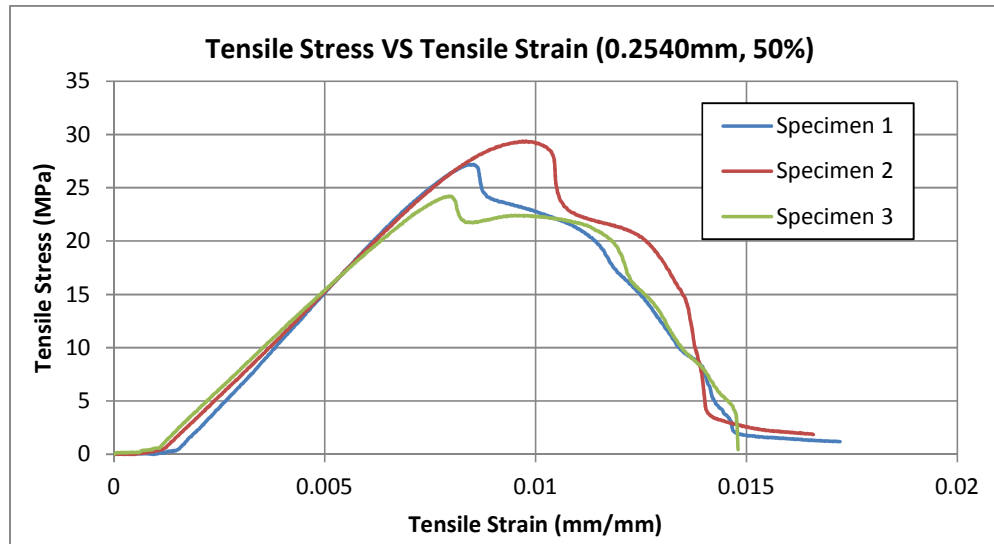


Figure 3: Tensile Stress - Strain Graph for Case 3 for Commercial FDM

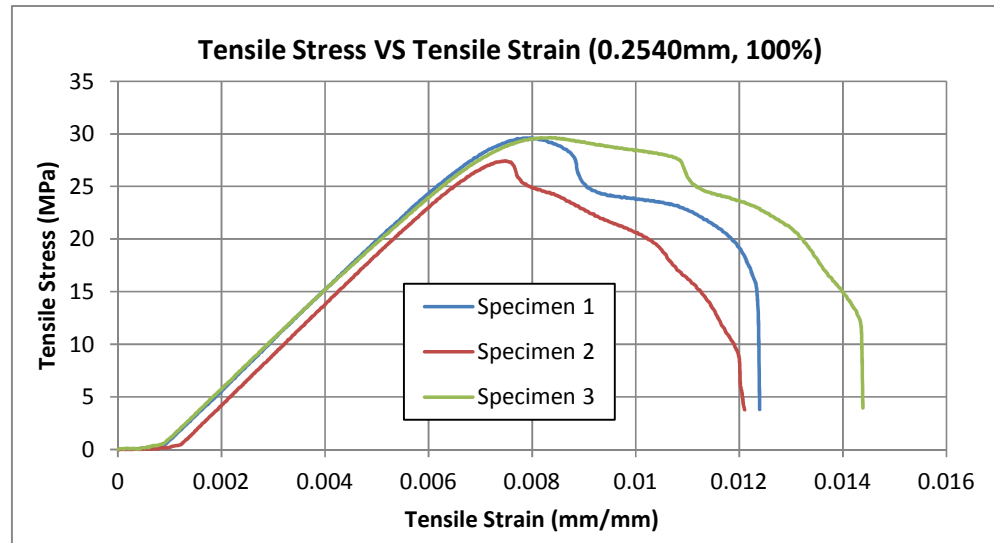


Figure 4: Tensile Stress - Strain Graph for Case 4 for Commercial FDM

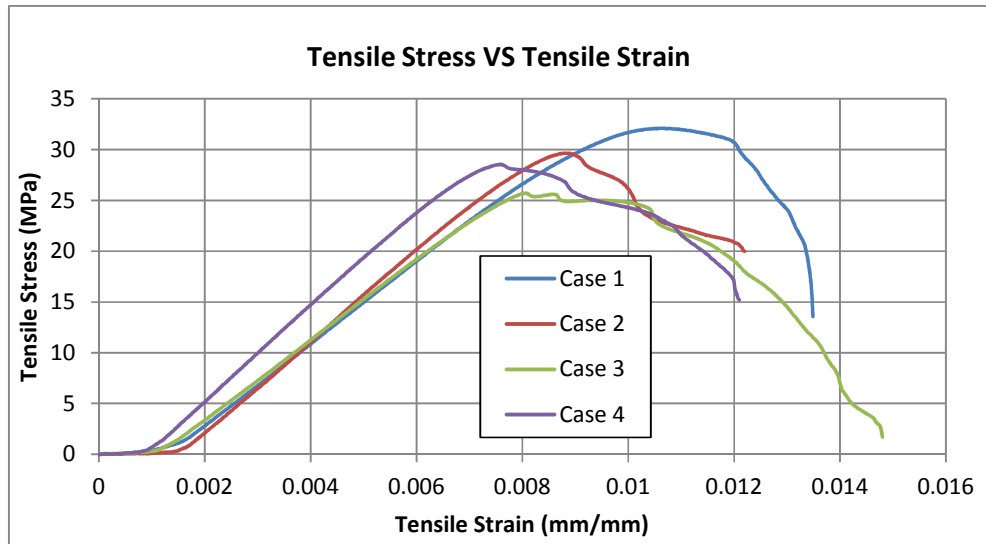


Figure 5: Average Tensile Stress - Strain Graph for All Cases for Commercial FDM

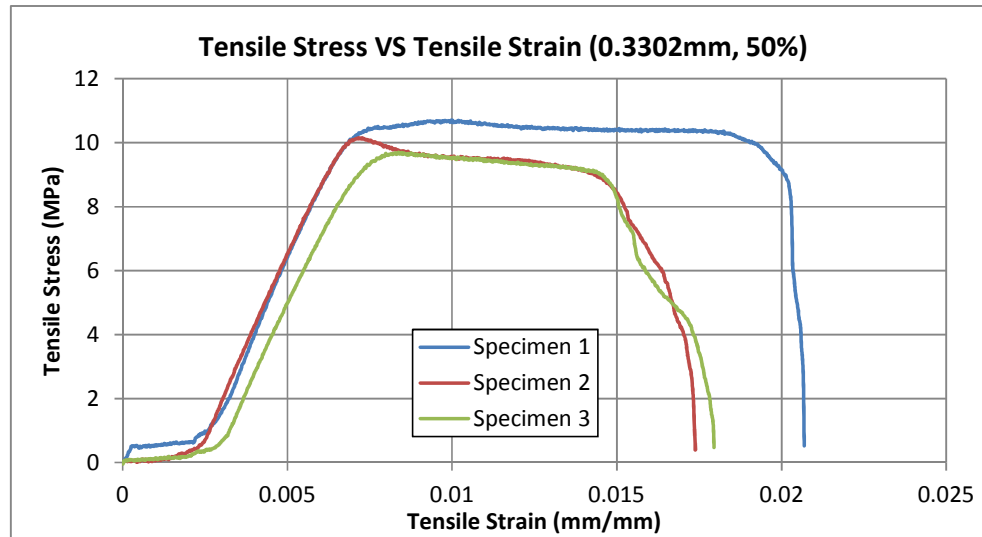


Figure 6: Tensile Stress - Strain Graph for Case 1 for Low-Cost FDM

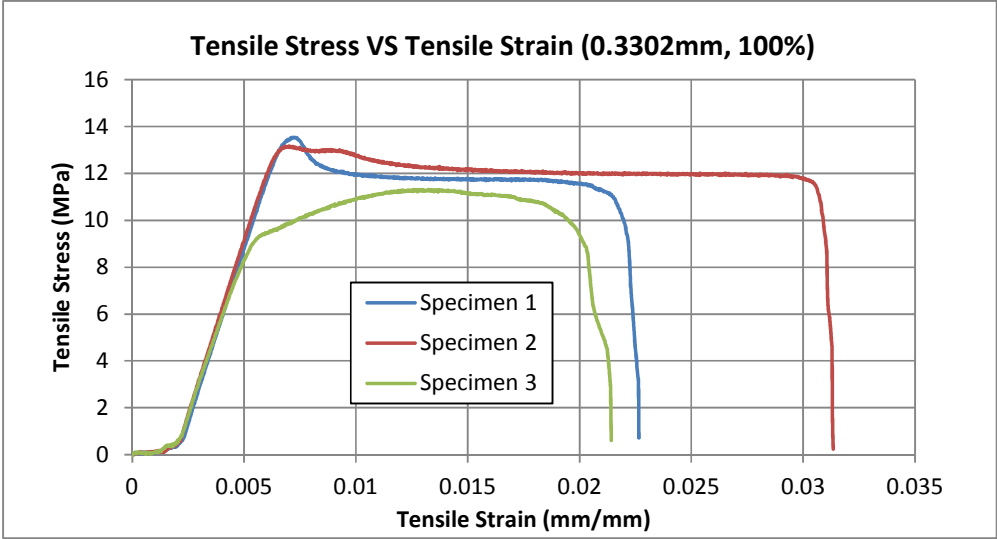


Figure 7: Tensile Stress - Strain Graph for Case 2 for Low-Cost FDM

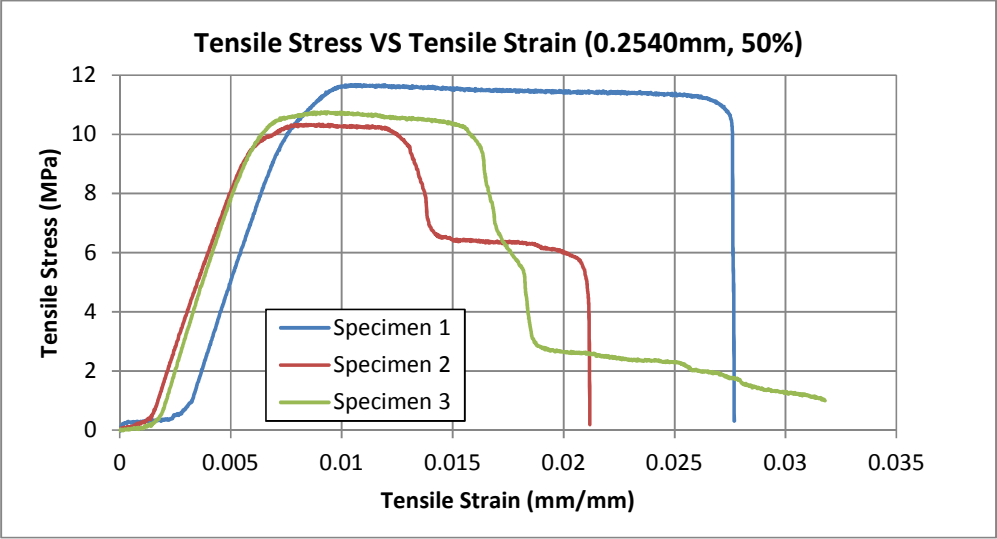


Figure 8: Tensile Stress - Strain Graph for Case 3 for Low-Cost FDM

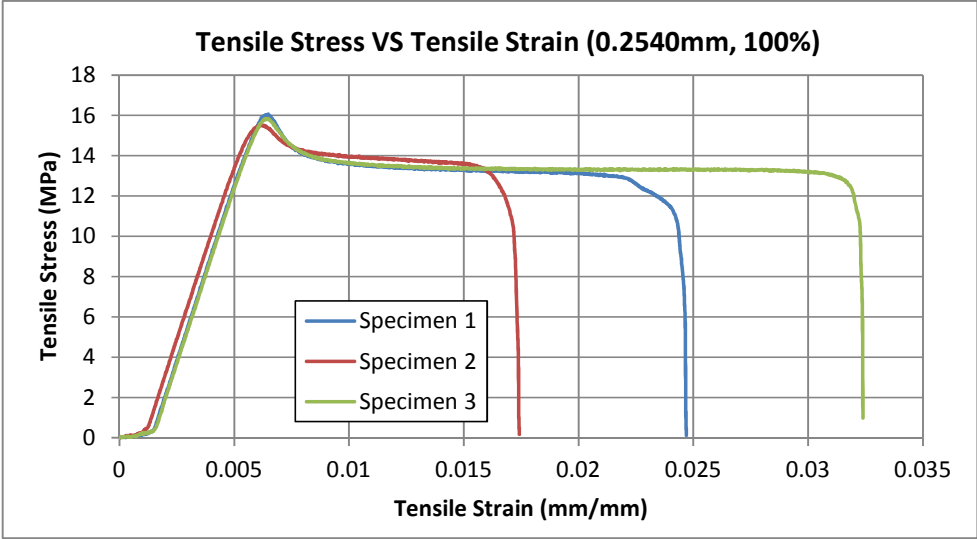


Figure 9: Tensile Stress - Strain Graph for Case 4 for Low-Cost FDM

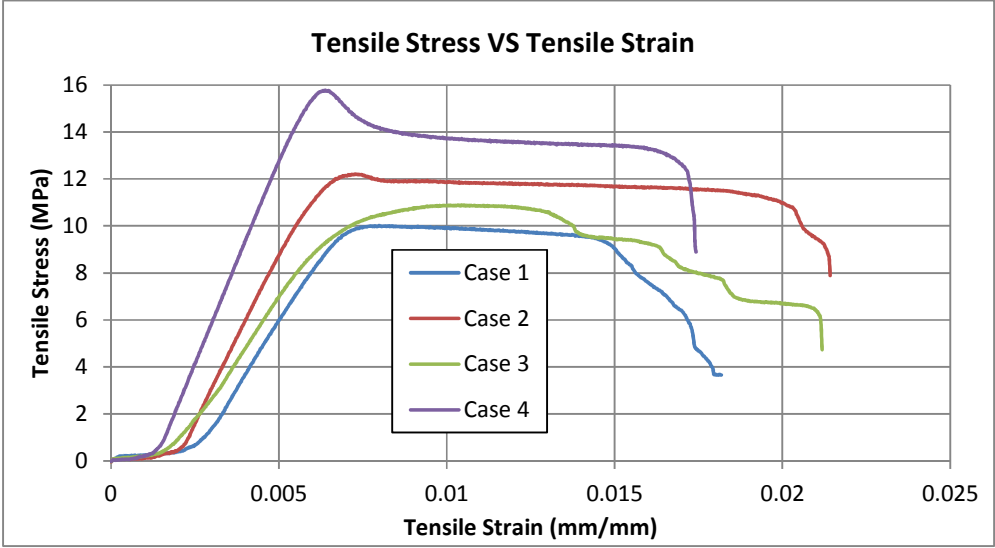


Figure 10: Average Tensile Stress - Strain Graph for All Cases for Low-Cost FDM

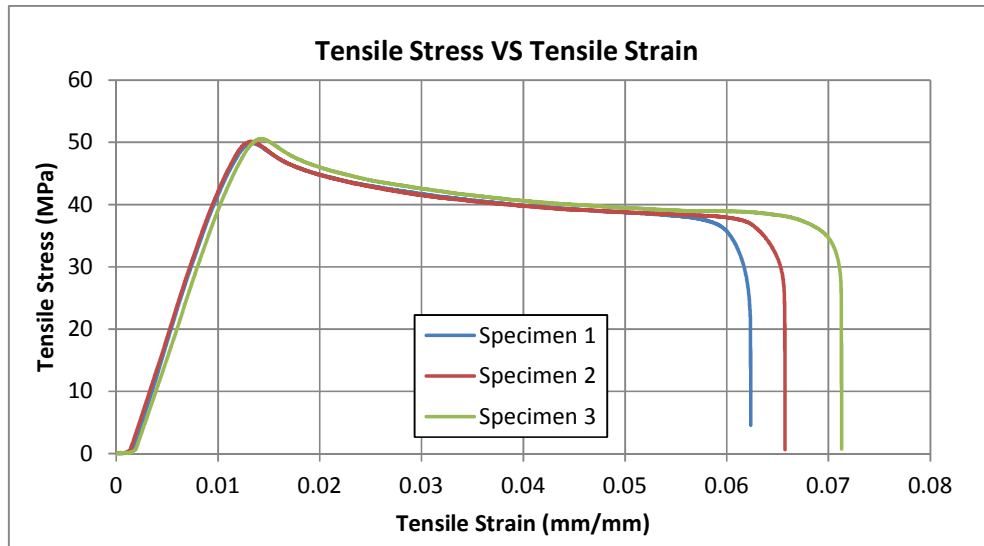


Figure 11: Tensile Stress - Strain Graph for Plastic Injection Molding

2) **Compression Test**

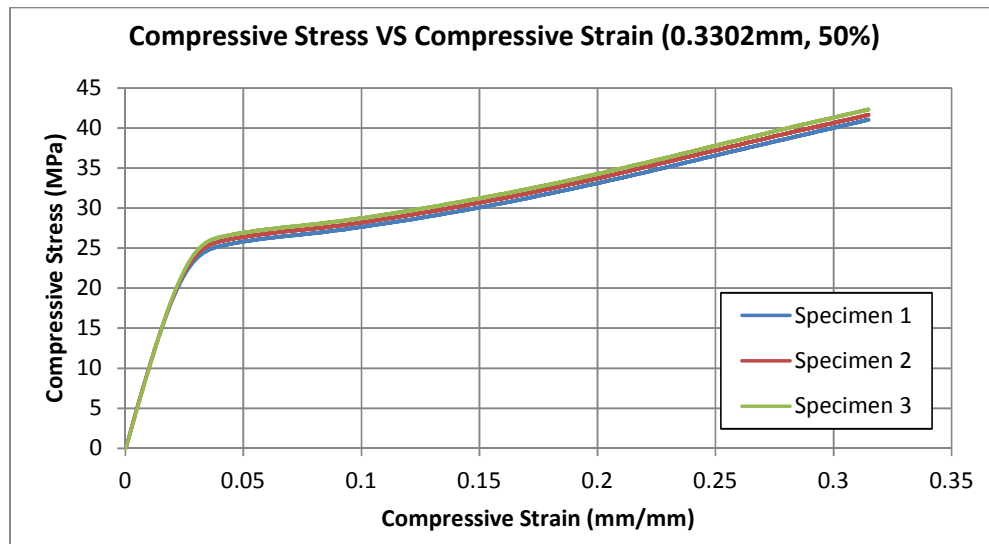


Figure 12: Compressive Stress - Strain Graph for Case 1 for Commercial FDM

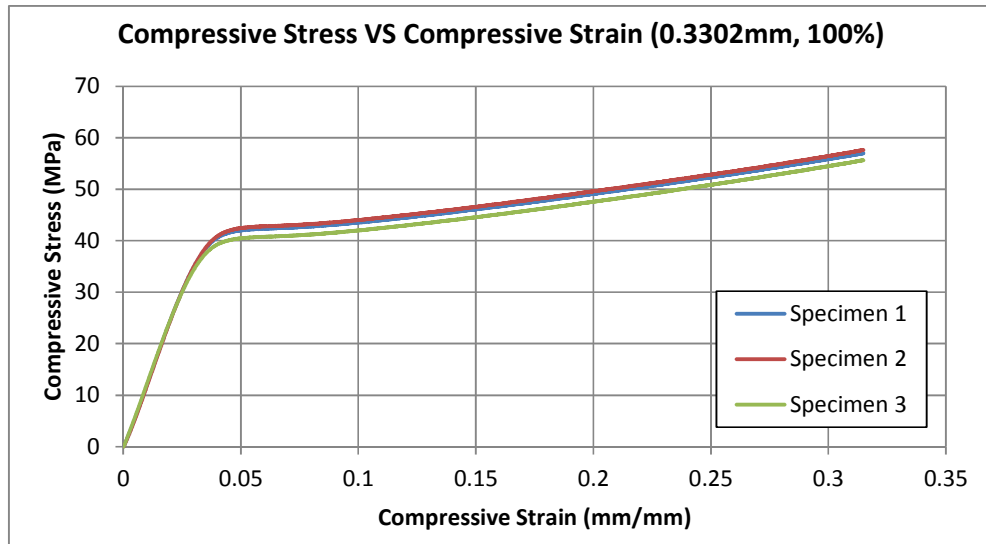


Figure 13: Compressive Stress - Strain Graph for Case 2 for Commercial FDM

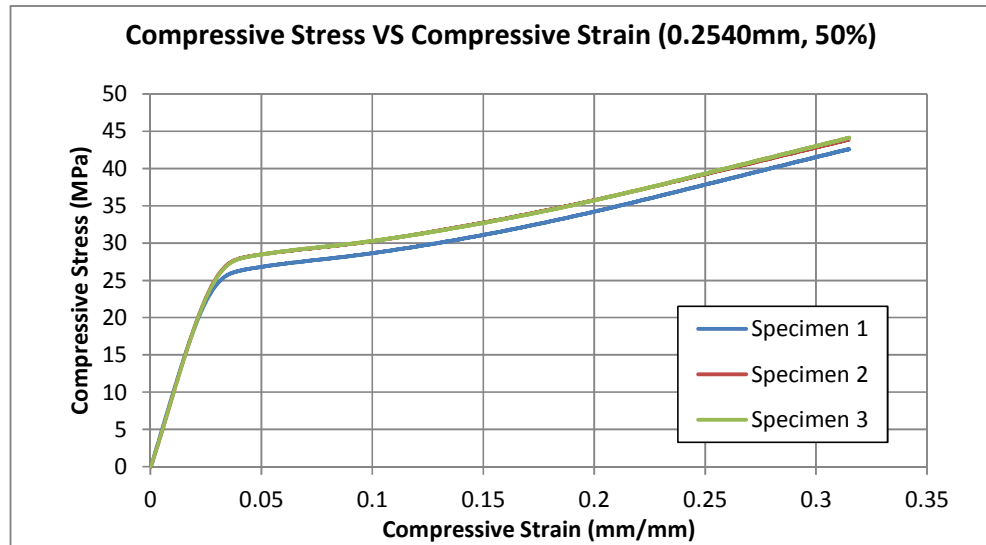


Figure 14: Compressive Stress - Strain Graph for Case 3 for Commercial FDM

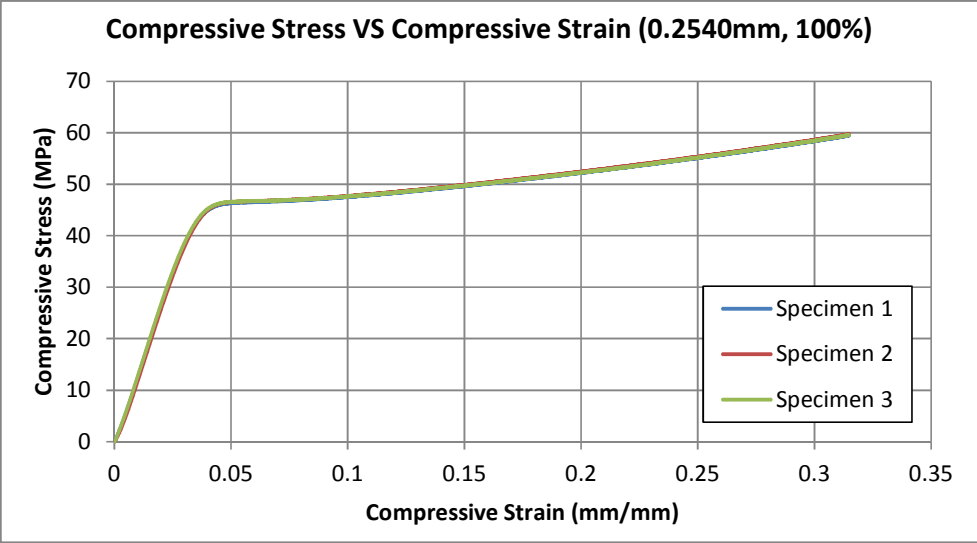


Figure 15: Compressive Stress - Strain Graph for Case 4 for Commercial FDM

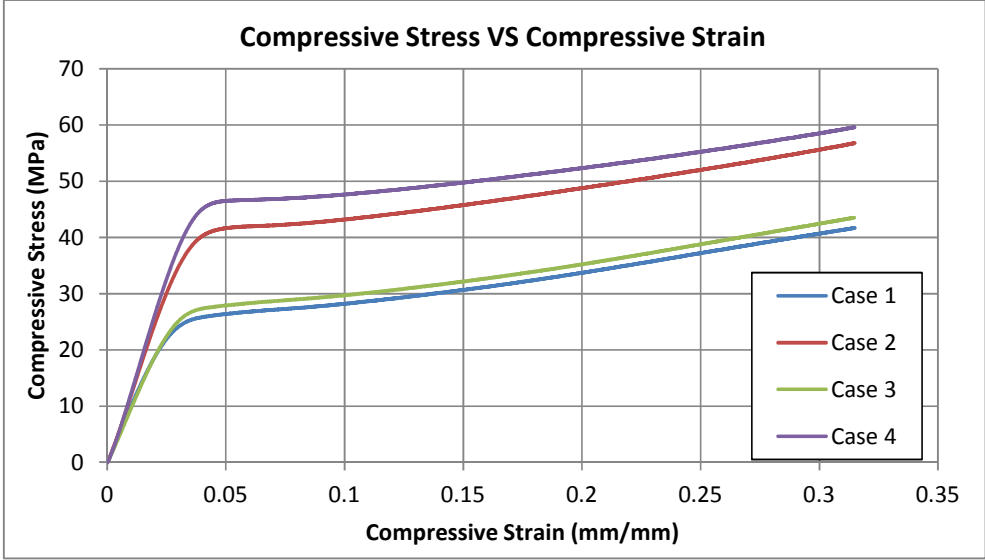


Figure 16: Average Compressive Stress - Strain Graph for All Cases for Commercial FDM

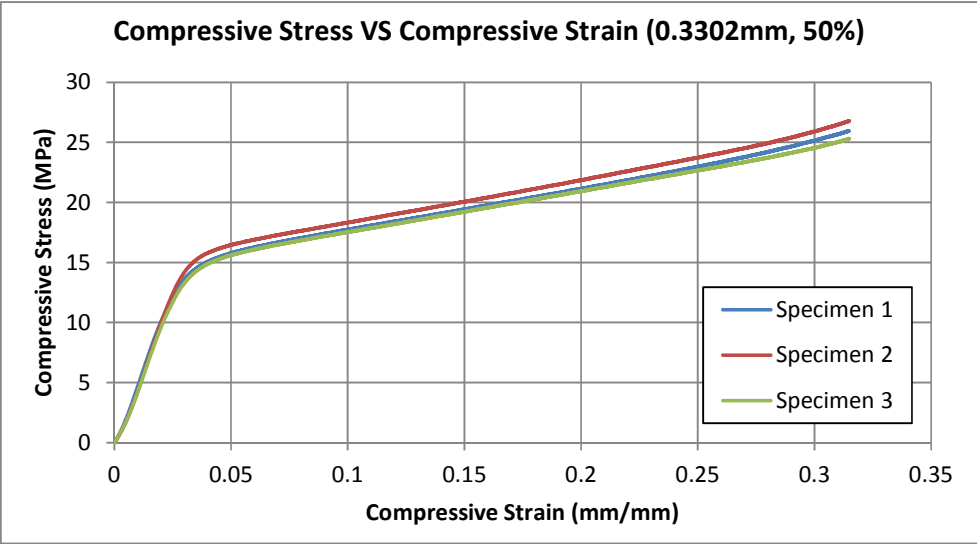


Figure 17: Compressive Stress - Strain Graph for Case 1 for Low-Cost FDM

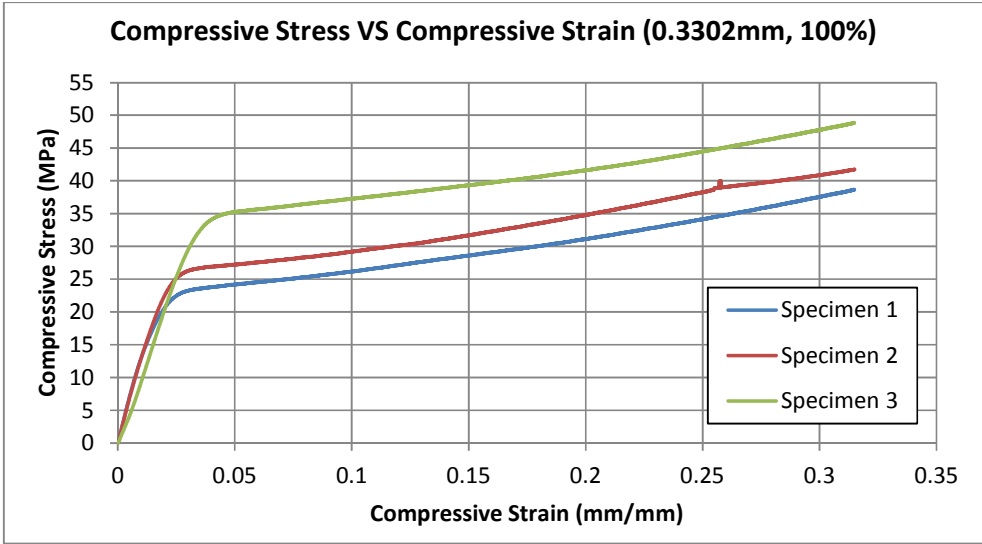


Figure 18: Compressive Stress - Strain Graph for Case 2 for Low-Cost FDM

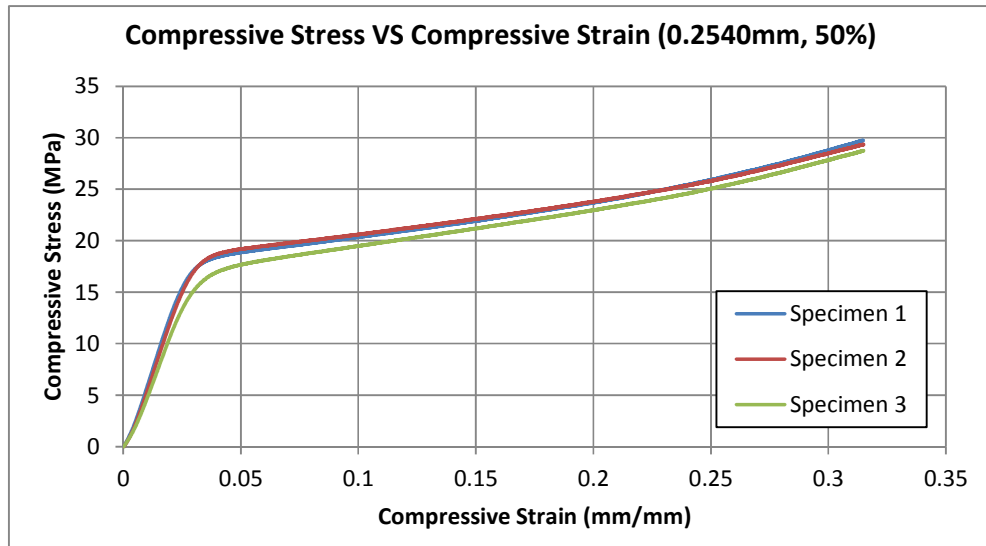


Figure 19: Compressive Stress - Strain Graph for Case 3 for Low-Cost FDM

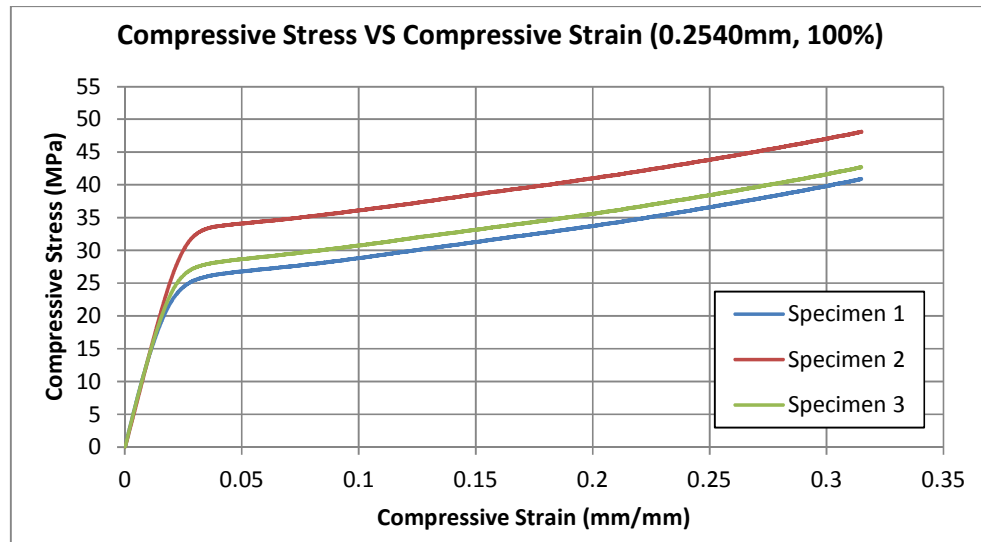


Figure 20: Compressive Stress - Strain Graph for Case 4 for Low-Cost FDM

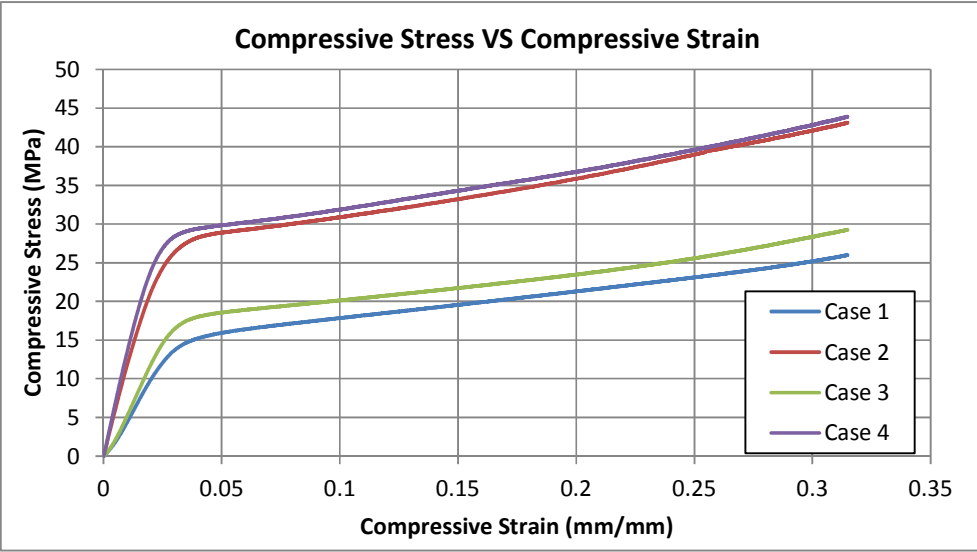


Figure 21: Average Compressive Stress - Strain Graph for All Cases for Low-Cost FDM